Determinants for Differential Effects on D-Ala-D-Lactate vs D-Ala-D-Ala Formation by the VanA Ligase from Vancomycin-Resistant Enterococci†

Ivan A. D. Lessard,‡,§ Vicki L. Healy,§ Il-Seon Park,|| and Christopher T. Walsh*

Department of Biological Chemistry and Molecular Pharmacology, Harvard Medical School, Boston, Massachusetts 02115

Received June 16, 1999

ABSTRACT: Bacteria with either intrinsic or inducible resistance to vancomycin make peptidoglycan (PG) precursors of lowered affinity for the antibiotic by switching the PG-D-Ala-D-Ala termini that are the antibiotic-binding target to either PG-D-Ala-D-lactate or PG-D-Ala-D-Ser as a consequence of altered specificity of the D-Ala-D-X ligases in the cell wall biosynthetic pathway. The VanA ligase of vancomycin-resistant enterococci, a D-Ala-D-lactate depsipeptide ligase, has the ability to recognize and activate the weak nucleophile D-lactate selectively over D-Ala_2 to capture the D-Ala_1-OPO_3^{2-} intermediate in the ligase active site. To ensure this selectivity in catalysis, VanA largely rejects the protonated (NH_3^+) form of D-Ala at subsite 2 (K_{M2} of 210 mM at pH 7.5) but not at subsite 1. In contrast, the deprotonated (NH_2) form of D-Ala (K_{M2} of 0.66 mM, k_{cat} of 550 min^{-1}) is a 17-fold better substrate compared to D-lactate (K_M of 0.69 mM, k_{cat} of 32 min^{-1}). The low concentration of the free amine form of D-Ala at physiological conditions (i.e., 0.1% at pH 7.0) explains the inefficiency of VanA in dipeptide synthesis. Mutational analysis revealed a residue in the putative ω-loop region, Arg242, which is partially responsible for electrostatically repelling the protonated form of D-Ala_2. The VanA enzyme represents a subfamily of D-Ala-D-X ligases in which two key active-site residues (Lys215 and Tyr216) in the active-site ω-loop of the *Escherichia coli* D-Ala-D-Ala ligase are absent. To look for functional complements in VanA, we have mutated 20 residues and evaluated effects on catalytic efficiency for both D-Ala-D-Ala dipeptide and D-Ala-D-lactate depsipeptide ligation. Mutation of Asp232 caused substantial defects in both dipeptide and depsipeptide ligase activity, suggesting a role in maintaining the loop position. In contrast, the H244A mutation caused an increase in K_{M2} for D-lactate but not D-Ala, indicating a differential role for His244 in the recognition of the weaker nucleophile D-lactate. Replacement of the VanA ω-loop by that of VanC2, a D-Ala-D-Ser ligase, eliminated D-Ala-D-lactate activity while improving by 3-fold the catalytic efficacy of D-Ala-D-Ala and D-Ala-D-Ser activity.

Development of resistance to the glycopeptide antibiotic vancomycin has become widespread over the past decade, and the vancomycin-resistant enterococci (VRE)[1] have emerged as significant opportunistic pathogens in nosocomial infections (*1*−*4*). The vancomycin group of antibiotics act on Gram-positive bacteria by targeting the D-alanyl-D-alanine (D-Ala-D-Ala) dipeptide moiety at the termini of peptidoglycan (PG) precursors and, in antibiotic-PG strand complexes, preventing the transpeptidative cross-linking of adjacent peptide and glycan strands that leads to a mechanically strong cell wall. Analysis of the molecular basis of vancomycin resistance has revealed three clinical phenotypes, designated as VanA, VanB, and VanC phenotypes with the first two more common than VanC (*5*, *6*). In both VanA and VanB phenotypes, the structural determinant of resistance is a switch from a terminal D-Ala-D-Ala dipeptide to a terminal D-alanyl-D-lactate (D-Ala-D-lactate) depsipeptide in peptidoglycan biosynthesis (*7*−*13*). In VanC, it is a swap from D-Ala-D-Ala to D-alanyl-D-serine (D-Ala-D-Ser) in the same PG pathway (*14*). For PG strands bearing D-Ala-D-lactate termini in place of D-Ala-D-Ala, there is a 1000-fold drop in affinity for binding vancomycin (*8*), while the D-Ala-D-Ser termini have a 6-fold decrease in affinity (*15*), and these effects are mirrored by rises in the minimal inhibitory concentration levels for vancomycin in the three clinical phenotypes (*9*, *16*).

Thus, the three VRE clinical phenotypes have in common the reprogramming of the D-Ala-D-Ala peptidoglycan terminus to a D-Ala-D-X linkage (X = lactate or serine), and this arises from molecular changes in the D-Ala-D-X ligases. In sensitive Gram-positives (staphylococci, streptococci, and enterococci), the dipeptide ligases make D-Ala-D-Ala, but in the VRE, these ligases show gain of function to produce either D-Ala-D-lactate (VanA and VanB) or D-Ala-D-Ser

† This research was supported by NIH Grant GM44338 to C.T.W.

* To whom correspondence should be addressed. Phone: (617) 432-1715. Fax: (617) 432-0438. E-mail: walsh@walsh.med.harvard.edu.

‡ Present address: Department of Biological Sciences, Boehringer Ingelheim (Canada) Ltd., Bio-Mèga Research Division, Laval, Quèbec, Canada H7S 2G5.

§ These authors have contributed equally.

|| Present address: Center for Cell Signaling Research and Department of Chemistry, Ewha University, Seoul 120-750, Korea.

[1] Abbreviations: D-Ala, D-alanine; D-F-Ala, 3-fluoro D-Ala; D-F_2-Ala, 3,3-difluoro D-Ala; D-F_3-Ala, 3,3,3-trifluoro D-Ala; D-Ala-D-Ala, D-alanyl-D-alanine dipeptide; D-Ala-D-lactate, D-alanyl-D-lactate depsipeptide; D-Ala-D-Ser, D-alanyl-D-serine dipeptide; D-Ser, D-serine; DdlB, *Escherichia coli* D-Ala-D-Ala ligase; LmDdl2, *Leuconostoc mesenteroides* D-Ala-D-lactate ligase; PCR, polymerase chain reaction; PG, peptidoglycan; SOE, splicing by overlap extension; TCL, thin-layer chromatography; VanA, *Enterococcus faecium* D-Ala-D-lactate ligase; VanC2, *Enterococcus casseliflavus* D-Ala-D-Ser ligase; VRE, vancomycin-resistant enterococci.

10.1021/bi991384c CCC: $18.00
Published on Web 09/29/1999

(VanC) as shown by expressing the D-Ala-D-X ligases from VanA (*17*), VanB (*18*), and a VanC (*19*) type of resistant enterococci and validating the D-Ala-D-lactate or D-Ala-D-Ser activity. The new ability to condense D-lactate is paralleled by rejection of D-Ala_2 by the VanA/B ligases. We show here that VanA discriminates against the zwitterionic form of D-Ala_2 that is the bulk species in solution at physiological pH.

To understand the basis of D,D-ligase specificity, Fan et al. (*20*) have previously reported the X-ray structure of the *Escherichia coli* DdlB D-Ala-D-Ala ligase and a Y216F mutant with a partial gain of function of D-Ala-D-lactate depsipeptide synthetase activity (*17*). Both were in complex with a potent, slow binding phosphinate inhibitor that becomes phosphorylated by ATP to yield a phosphinophosphate ligand that is a close analogue of a tetrahedral intermediate in the normal catalytic cycle, allowing definition of the active-site region. To date, there are no crystal structures of any of the VRE D-Ala-D-X ligases, so we have used the *E. coli* DdlB structure for extrapolation and guidance of mutagenesis in VanA and VanC ligases. The *E. coli* DdlB structure revealed two loops that closed over the bound phosphinophosphate and ADP (Figures 1 and 2). The first loop (the 150S loop) is part of a X-Gly-Ser-Ser-X-Gly motif that is conserved among all D-Ala-D-X ligases and contains the Ser150 residue which is part of an hydrogen-bonding triad that orients the Glu15 for binding the first D-Ala and is believed to hold the second loop in place. The second loop, called the ω-loop, forms a short helix spanning residues 210−217 closed down over the bound ADP and reaction intermediates during catalysis but is believed to be flexible and exposed in the absence of substrates (*20*). When some key residues in the ω-loop were analyzed by mutagenesis, the K215A enzyme had dramatically decreased activity, consistent with a role in stabilizing the γ-PO_3^{2-} of ATP in phosphoryl transfer (*21*), and the Y216F mutant had a partial gain of depsipeptide synthetase function (*17*). However, no corresponding lysine and phenylalanine residues have been identified in VanA.

When the D-Ala-D-X superfamily of bacterial ligases is compared by homology analysis, five subfamilies can be distinguished: two that are D-Ala-D-Ala ligases physiologically, two that are D-Ala-D-lactate ligases, and one D-Ala-D-Ser ligase subfamily (Figure 3). Except for the lysine and phenylalanine/tyrosine residues of the ω-loop that are absent in the VanA subfamily, the other key catalytic and binding residues that defined the DdlB active site are highly conserved among the entire Ddl family (Figure 2A). The D-Ala-D-Ala and D-Ala-D-Ser ligase (VanC) subfamilies show high homology, including the conservation of residues and the projected size of the ω-loop (Figures 1 and 2). Of the two D-Ala-D-lactate ligase subfamilies, one represented by the *Leuconostoc mesenteroides* Ddl (LmDdl2) has a comparable ω-loop, while the second, represented by the VanA and VanB ligases and the DdlM from the antibiotic producer, *Streptomyces toyocaensis*, clearly does not have a comparable pattern of conserved residues (Figure 1D). We have previously shown that the LmDdl2, with phenylalanine corresponding to Tyr216 of *E. coli* DdlB, when mutated to produce a F261Y mutant, has suppressed depsipeptide ligase activity while retaining D,D-dipeptide ligase activity (*17*). These data reinforced the role of tyrosine/phenylalanine in the ω-loop (e.g., of DdlB and of LmDdl2) as a dipeptide/depsipeptide synthesis determinant and the ability to vary the two activities differentially. Given the importance of the ω-loop and the variability in at least two consequential residues between the Ddls and the VanA and VanB D,D-ligases (lysine and phenylalanine/tyrosine residues), we have sought to find loop residues in VanA that would define a comparable role in the VRE family of D-Ala-D-X ligases and report such results here.

MATERIALS AND METHODS

Materials. Bacteriological media were obtained from Difco Laboratories. Competent *E. coli* strain BL21 (DE3) [F-, *ompT*, *hsdS*$_B$, (r_{B-}, m_{B-}), *gal*, *dcm*, (DE3)] and expression vector pET28b(+) were purchased from Novagen. Competent *E. coli* strain DH5α [F^-, *ϕ*80d*lacZ*Δ*M15*, Δ(*lacZYA-argF*)*U169*, *deoR*, *recA1*, *endA1*, *hsdR17*(r_K^-, m_K^+), *phoA*, *supE44*, λ^-, *thi-1*, *gyrA96*, *relA1*] was purchased from GibcoBRL. Restriction endonucleases, T4 DNA ligase, and calf intestinal alkaline phosphatase were obtained from New England Biolabs. *Pfu* DNA polymerase was purchased from Stratagene. Isopropyl-1-thio-*β*-D-galactopyranoside and 3-monofluoro DL-Ala (DL-F-Ala) were purchased from Bachem Biosciences. Reduced nicotinamide adenine dinucleotide (NADH), L-lactate dehydrogenase, phosphoenolpyruvate, and pyruvate kinase were from Roche Molecular Biochemicals. D-[^{14}C]Ala, D-[^{14}C]lactate, and D-[^{14}C]Ser were from American Radiolabeled Chemicals Inc, α-[^{32}P]-ATP was from New England Nuclear, and thin-layer chromatography (TLC) cellulose, TLC silica, and TLC polyethyleneimine cellulose plates were from Kodak. Ampicilin, kanamycin, D-Ala, D-Ser, ATP, DL-hydroxybutyrate, and D-lactate were purchased from Sigma. 3,3-Difluoro D-Ala (D-F_2-Ala) was a kind gift from Merck & Co (Rahway). 3,3,3-Trifluoro DL-Ala (DL-F_3-Ala) was purchased from ABCR (Germany). D-Glyceric acid [40% (w/v) water] was purchased from TCI America. Ni-NTA superflow resin was purchased from Qiagen. Plasmid pVanC2 expressing the *vanC2* gene from *Enterococcus casseliflavus* has been described previously (*19*). Purified *L. mesenteroides* Ddl (LmDdl2) protein was obtained from earlier work (*17*). *E. coli* DdlB was purified as described previously (*21*).

Recombinant DNA Methods. Recombinant DNA techniques were performed as described elsewhere (*22*). Preparation of plasmid DNA, gel purification of DNA fragments, and purification of polymerase chain reaction (PCR) amplified DNA fragments (*23*, *24*) were performed using QIAprep spin plasmid miniprep kit, QIAEX II gel extraction kit and QIAquick PCR purification kit, respectively (Qiagen). PCRs were carried out as described by ref *25*, using the *Pfu* DNA polymerase. Splicing by overlap extension (SOE) reactions (*26*) was carried out as for the PCR using approximately an equimolar ratio (total amount ca. 50 ng) of each of the gel-purified PCR-amplified DNA fragments to be joined as template. The fidelity of the SOE- or PCR-amplified DNA fragments was established by nucleotide sequencing after subcloning into the expression vector. Oligonucleotide primers were obtained from Integrated DNA Technologies, and DNA sequencing was performed on double-stranded DNA by the Molecular Biology Core Facility of the Dana Farber Cancer Institute (Boston, MA).

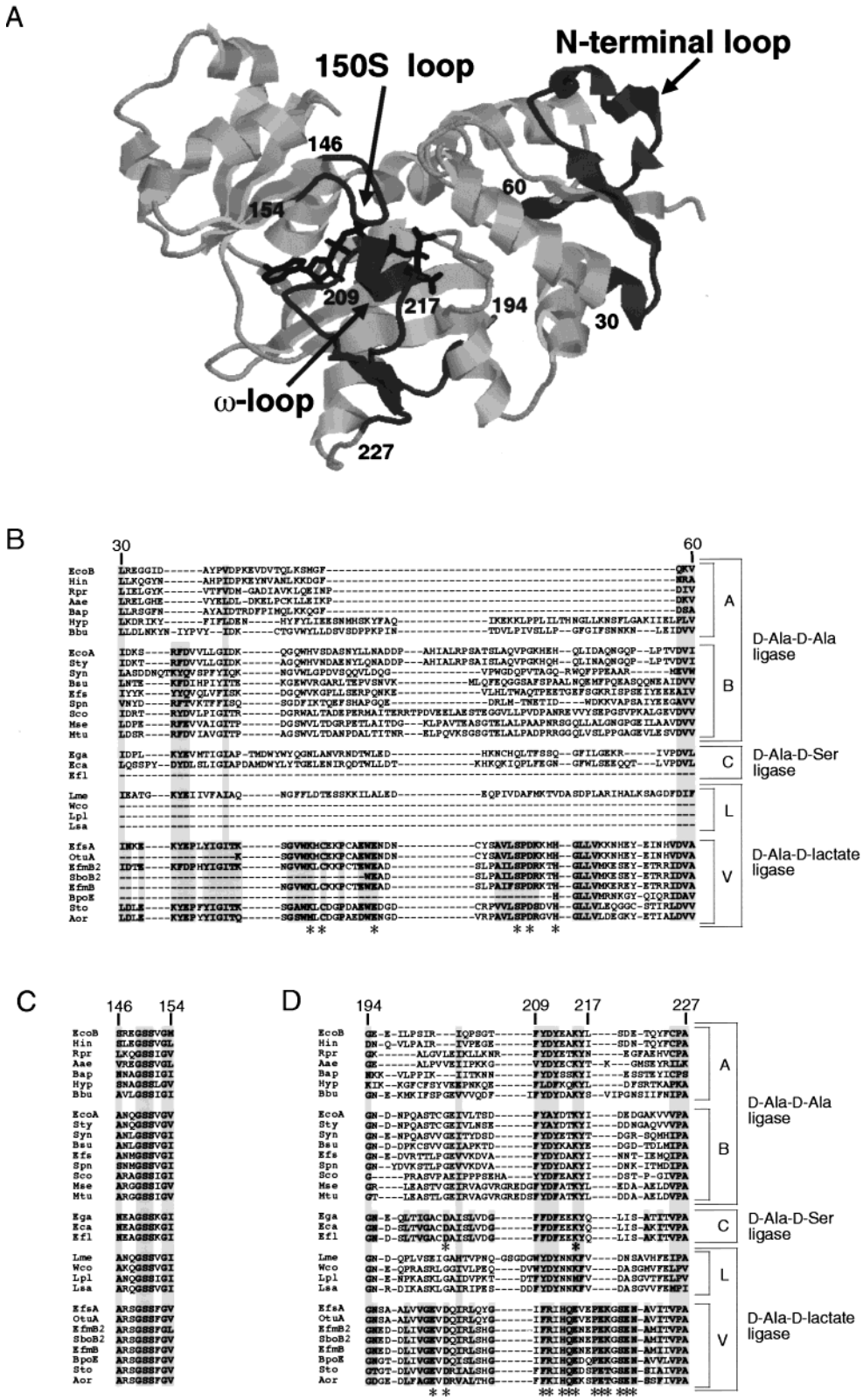

FIGURE 1: The structure of the *Escherichia coli* DdlB and partial sequence alignment of D-Ala-D-X ligases. (A) Cartoon view of the crystal structure of DdlB with the bound phosphinophosphate inhibitor and ADP shown in black (*20*). The numbers represent residues in DdlB. Sequence alignments of the highlighted regions (dark gray) are given in panels B−D. (B) Alignment of the N-terminal region of the ligases using Clustal W (*47*) followed by minor adjustments based on visual inspection of the alignment. The numbers refer to the positions of the amino acids in the primary sequence of DdlB. The subfamily designations are based on those of Figure 3 (A, DdlA group; B, DdlB group; C, VanC group; L, lactic acid bacteria group; V, VanA group). Highlighted boxes contain residues in a column that are at least 75% similar, and stars indicate residues in VanA or VanC2 that were mutated in this study. (C) Highly conserved sequence corresponding to the small loop (150S loop) in DdlB that closes over the active site in the presence of substrates. (D) Alignment of the sequences in and adjacent to the putative ω-loops. Critical residues for catalysis in DdlB are also indicated. Ser150 hydrogen bonds with Glu15 and Tyr216 to help orient the active site for catalysis (Figure 2B) (*20*). Lys215 stabilizes the γ-PO_3^{2-} of ATP in phosphoryl transfer (*21*), and Y216F DdlB gained some depsipeptide synthetase activity (Figure 2A) (*17*).

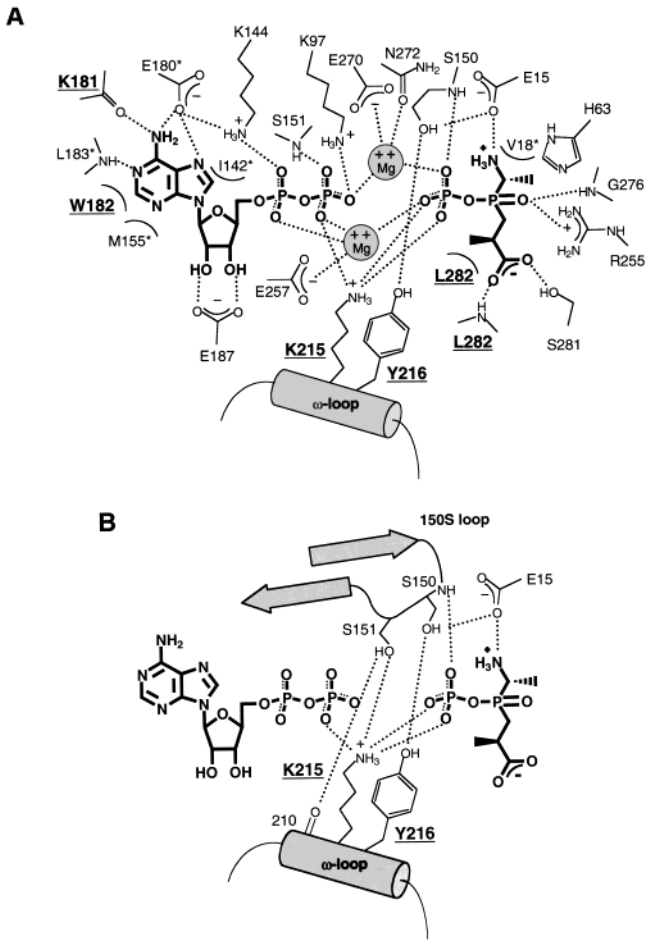

FIGURE 2: Active site of DdlB with bound ADP and phosphinophosphate inhibitor (*20*). (A) The residue numbers that are not underlined or starred correspond to amino acids in DdlB that are conserved in all D-Ala-D-X ligases. Stars indicate conservative changes, and bold and underlined indicate nonconserved residues. (B) The 150S loop containing the X-Gly-Ser-Ser-X-Gly motif that closes over the active site and supplies Ser150 for hydrogen bonding to Tyr216 in the ω-loop and Glu15 for recognition of the amino-terminal of D-Ala$_1$ (*20*).

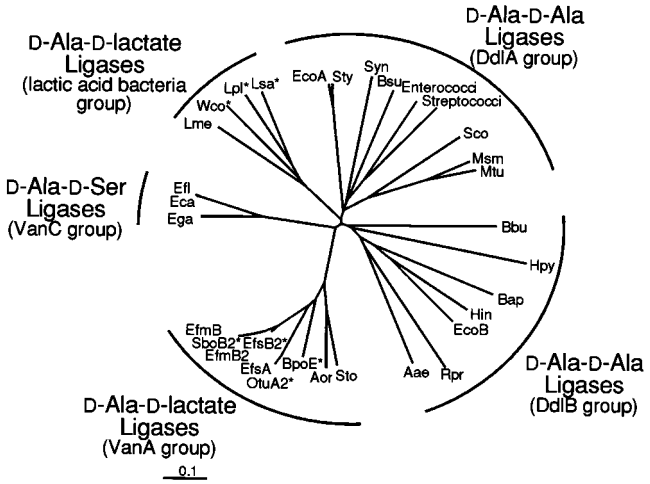

FIGURE 3: Phylogenetic tree of D-Ala-D-X ligase subfamilies. This alignment was obtained using the program Clustal W (*47*). Syn, *Synechocystis* sp.; Bsu, *Bacillus subtilis*; Enterococci, *Enterococcus* sp. (*Enterococcus faecalis*); Streptococci, *Streptococcus* sp. (*Streptococcus pneumonia*); Sco, *Streptomyces coelicolor*; Msm, *Mycobacterium smegmatis*; Mtu, *Mycobacterium tuberculosis*; Bbu, *Borrelia burgdoferi*; Hpy, *Helicobacter pylori*; Bap, *Buchnera aphidicola*; Hin, *Haemophilus influenzae*; EcoB, *Escherichia coli* (*ddlB*); Rpr, *Rickettsia prowazekii*; Aae, *Aquifex aeolicus*; Sto, *Streptomyces toyocaensis* (*ddlM*); Aor, *Amycolatopsis orientalis* (*ddlN*); BpoE, *Bacillus popilliae* (*vanE*); OtuA2, *Oerskovia turbata* (*vanA2*); EfsA, *Enterococcus faecium* (*vanA*); EfmB2, *Enterococcus faecium* (*vanB2*); EfsB2, *Enterococcus faecalis* (*vanB2*); SboB2, *Streptococcus bovis* (*vanB2*); EfmB, *Enterococcus faecium* (*vanB*); Ega, *Enterococcus gallinerum* (*vanC*); Eca, *Enterococcus casseliflavus* (*vanC2*); Efl, *Enterococcus flavescens* (VanC3); Lme, *Leuconostoc mesenteroides*; Wco, *Weassella confusa*; Lpl, *Lactobacillus plantarum*; Lsa, *Lactobacillus salivarius*; EcoA, *Escherichia coli* (*ddlA*); Sty, *Salmonella typhimurium*. For the DdlA group, all the enterococci species were very closely related; therefore, the *Enterococcus faecalis* sequence was taken as a representative of this genius. Similarly, the *Streptococcus pneumonia* sequence was chosen among the streptococcal genus. Stars refer to alignments based on incomplete sequences.

Construction of a His$_6$-tag Fusion for VanA purification. The gene encoding enterococcal VanA was PCR-amplified from pIADL1 (IADL and CTW unpublished vector) using the primer pair 2007/1028 (Table 1). The purified PCR-amplified DNA fragment was subcloned into pET28b(+) at the *Nde*I and *Eco*RI restriction sites. The resulting plasmid (pIADL54) encodes an His$_6$−VanA protein with a thrombin cleavage site allowing selective removal of the His$_6$-tag if desired.

Site-Directed Mutagenesis. Site-directed mutants were constructed by PCR mutagenesis using the SOE method. For the construction of mutants of VanA (plasmid pIADL54) and VanAωC2(S) (plasmid pIADL118, see below), in the first round of PCR, the sequence upstream and downstream of the mutation was amplified separately using pIADL54 (pIADL118) as template and the sense/antisense primer pairs 2031/11XX and 21XX/1028, respectively, except for the VanA mutants K50A, C52A, E60A, D72A and H76A which was amplified using the sense/antisense primer pairs 2092/11XX and 21XX/1092, respectively (Table 1, each mutant corresponds to a particular XX pair of primers). The resulting PCR-amplified DNA fragments were gel purified and subjected to a second round of PCR using the 2092/1092 primer pair for the VanA mutants K50A, C52A, E60A, D72A, and H76A and the 2031/1028 primer pair for the remaining VanA and VanAωC2(S) mutants. The purified SOE-amplified DNA fragment was subcloned into pIADL54 at the *Nde*I/*Bam*HI restriction sites for the VanA mutants K50A, C52A, E60A, D72A, and H76A and at the *Bam*HI/*Eco*RI restrictions for the remaining VanA and VanAωC2(S) mutants. For the construction of mutants of VanC2 (plasmid pVanC2) and VanC2ωA(L) (plasmid pIADL122 and pIADL122.H320Y.A325R, see below), the sequence upstream and downstream of the mutation was amplified separately using pVanC2 (pIADL122, pIADL122.H320Y.A325R) as template and the sense/antisense primer pairs 2099/11XX and 21XX/1099, respectively. The resulting PCR-amplified DNA fragments were gel purified and subjected to a second round of PCR using the 2099/1099 primer pair. The purified SOE-amplified DNA fragment was subcloned into pVanC2 at the *Bst*BI and *Bam*HI restrictions sites.

ω-Loop Exchange between VanC2 and VanA Proteins by Mutagenesis. The stretch of amino acid in and around the putative ω-loop of VanA (plasmid pIADL54) and VanC2 (plasmid pVanC2) were swapped between the respective proteins into two different lengths by PCR mutagenesis using the SOE method. For the smaller version of ω-loop exchange [VanAωC2(S) and VanC2ωA(S), see Figure 8B], in the first

Table 1: Oligonucleotide Primers for Site-Directed Mutagenesis and ω-Loop Replacement[a]

comment	code	5′-3′ nucleotide sequence
VanA$_{NdeI}$	2007	**CCTCTAGACAGGAGACCAT**ATGAATAGAATAAAAGTTGCAATACTG
VanA$_{EcoRI}$	1028	**GGGAATTCACGCG**TTATCACCCCTTTAACGCTAATACG
VanA$_{internal}$	2031	GCTATTCAGCTGTACTCTCG
T7$_{promoter}$	2092	AAGGAGATATACCATGGGCAGC
VanA$_{internal}$	1092	TTCGCAACGATGTATGTCAAC
K50A	2144	GGTGTATGG**GC**AATGTGCGAAAAACCT
K50A	1144	GTTTTTCGCACATT**GC**CCATACACCAG
C52A	2143	GTATGGAAAATG**GCC**GAAAAACCTT
C52A	1143	AAGGTTTTTC**GGC**CATTTTCCATAC
E60A	2145	GGAATGGG**C**AAACGACAATTGCT
E60A	1145	TAGCAATTGTCGTTT**G**CCCATTCC
S70A	2152	GTACTC**GCA**CCGGATAAAAAAATGC
S70A	1152	CATTTTTTTATCCGG**TGC**GAGTACAGC
D72A	2146	GTACTCTCGCCGG**C**TAAAAAAATGC
D72A	1146	GCATTTTTTTA**G**CCGGCGAGAGTACA
H76A	2147	GGATAAAAAAATG**GC**CGGATTACTTGTTA
H76A	1147	TAACAAGTAATCCG**GC**CATTTTTTTATCC
E230A	2149	GTTGTTGGC**GCA**GTGGACCAAATCAG
E230A	1149	CTGATTTGGTCCAC**TGC**GCCAACAAC
D232A	2150	GTTGGCGAGGTG**GCC**CAAATCAGGCT
D232A	1150	AGCCTGATTTG**GGC**CACCTCGCCAAC
Q233A	2151	GGTGGAC**GCA**ATCAGGCTGCAGT
Q233A	1151	ACTGCAGCCTGAT**TGC**GTCCACCTCG
F241A	2148	CAGTACGGAATC**GCT**CGTATTCATCAGG
F241A	1148	GATGAATACG**AGC**GATTCCGTACTGC
F241Y	2142	CAGTACGGAATC**TAT**CGTATTCATCAGG
F241Y	1142	GATGAATACG**ATA**GATTCCGTACTGC
R242A	1154	GATGAAT**TGC**AAAGATTCCGTACTGC
R242A	2154	CAGTACGGAATCTTT**GCA**ATTCATCAGG
R242A.H244A	1155	CGACTTCCTG**TGC**AAT**TGC**AAAGATTC
R242A.H244A	2155	GAATCTTT**GCA**ATT**GCA**CAGGAAGTCG
Q245A	2118	GAATCTTTCGTATTCAT**GCG**GAAGTCGAGC
Q245A	1118	CTCGACTTC**CGC**ATGAATACGAAAGATTCC
E246A	2119	CATCAG**GCA**GTCGAGCCGGAAAAAGG
E246A	1119	CCTTTTTCCGGCTCGAC**TGC**CTGATGAATACG
P249A	2121	CGAG**GCG**GAAAAAGGCTCTGAAAACG
P249A	1121	CGTTTTCAGAGCCTTTTTC**CGC**CTCGACTTCC
E250A	2120	CGAGCCG**GCA**AAAGGCTCTGAAAACG
E250A	1120	CGTTTTCAGAGCCTTT**TGC**CGGCTCGACTTCC
K251A	2137	CGAGCCGGAA**GCA**GGCTCTGAAAACG
K251A	1137	CGTTTTCAGAGCC**TGC**TTCCGGCTCGACTTCC
S253A	2138	GGAAAAAGGC**GCT**GAAAACGCAGTT
S253A	1138	CTGCGTTTTC**AGC**GCCTTTTTCCGGCTCGAC
E254A	2139	GGAAAAAGGCTCT**GCA**AACGCAGTTATAACC
E254A	1139	CTGCGTT**TGC**AGAGCCTTTTTCC
N255A	2140	GCTCTGAA**GCC**GCAGTTATAACC
N255A	1140	GGTTATAACTGC**GGC**TTCAGAGCCTTTTTCC
R317M	2141	GTCATACAGT**ATG**TATCCCCGTATGATG
R317M	1141	CATACGGGGATA**CAT**ACTGTATGACGTG
T7$_{terminator}$	1099	AAGGGGTTATGCTAGTTATTGC
VanC2$_{internal}$	2099	AACAGAAAATACAGCCGCTATTCG
D241A[b]	1157	CTAATGAAATGGCG**G**CACAAGCACCGACAG
D241A[b]	2157	GGTGCTTGTG**C**CGCCATTTCATTAGTAGAC
K255A[b]	1156	TGATCAGCTGGTA**GGC**TTCTTCAAAATCG
K255A[b]	2156	CGATTTTGAAGAA**GCC**TACCAGCTGATCA
small loop VanC	1sl-C	cagctggtacttttcttcaaaatcgaaaaaTCCGTACTGCAGCCTGATTTGGTC
small loop VanC	2sl-C	cgattttgaagaaaagtaccagctgatcagcGCAGTTATAACCGTTCCCGCAGAC
large loop VanC	1bl-C1	ctactaatgaaatggcgtcacaagcGCCAACAACTAACGCGGCACTGTTTCC
large loop VanC	1bl-C2	cttcaaaatcgaaaaagccgtctactaatgaaatggcgtcac
large loop VanC	2bl-C1	gaaaagtaccagctgatcagcgccaaaATAACCGTTCCCGCAGACCTTTCAGC
large loop VanC	2bl-C2	gacggctttttcgattttgaagaaaagtaccagctgatc
small loop VanA	1sl-A	cttttttccggctcgacttcctgatgaatacgaaagatgccgtctactaatgaaatggcgtcacaag
small loop VanA	2sl-A	catcaggaagtcgagccggaaaaaggctctgaaaacgccaaaatcaccgtccctgcgccattg
large loop VanA	1bl-A3	tactgcagcctgatttggtccacctcaccgacagtcaaagagtcgttgc
large loop VanA	2bl-A3	aggtggaccaaatcaggctgcagtacggaatctttcgtattcatcaggaag
H320Y.A325R[c]	1098	CCATCATG**CG**AGGATAGCGGGAGT**A**ACTCGTAA
H320Y.A325R[c]	2098	GT**T**ACTCCCGCTATCCT**CG**CATGATGGCAGCG
Y247F[b]	1153	TGATCAGCTGG**A**ACTTTTCTTCAAAATCG
Y247F[b]	2153a	CGATTTTGAAGAAAAGT**T**CCAGCTGATCAGCGCAGT
K246A[b]	1156	TGATCAGCTGGTA**GGC**TTCTTCAAAATC
K246A[b]	2156a	CGATTTTGAAGAA**GCC**TACCAGCTGATCAGCGCAGT

[a] Mismatch mutations are underlined and in bold; ω-loop swap between the *vanA* and *vanC2* genes are in lower case and underlined. [b] VanC2 mutations. [c] VanC2ωA mutations.

round of PCR, the sequence upstream and downstream coding for the stretch of amino acid to be swapped was amplified separately using pIADL54 or pVanC2 as template and the sense/antisense primer pairs 2031/1sl-C and 2sl-C/1028 (pIADL54) or 2099/1sl-A and 2sl-A/1099 (pVanC2), respectively (Table 1). The resulting PCR-amplified DNA fragments were gel purified and subjected to a second round of PCR using the 2031/1028 [VanAωC2(S)] or 2099/1099 [VanC2ωA(S)] primer pair. The purified SOE-amplified DNA fragment was subcloned into pIADL54 at the *Bam*HI and *Eco*RI restriction sites creating plasmid pIADL118 [VanAωC2(s)] or into pVanC2 at the *Bst*BI and *Bam*HI restriction sites creating plasmid pIADL121 [VanC2ωA(S)]. For the larger version of the ω-loop exchange of VanC2 replacing the one in the VanA protein [VanAωC2(L), see Figure 8B], the first round of PCR was conducted as described above using the sense/antisense primer pairs 2031/1bl-C1 and 2bl-C1/1028 (pIADL54). The two PCR products were reamplified using the primer pairs 2031/1bl-C2 and 2bl-C2/1028, respectively. The resulting PCR-amplified DNA fragments were gel purified and subjected to a third round of PCR using the 2031/1028 primer pair. The purified SOE-amplified DNA fragment was subcloned into pIADL54 at the *Bam*HI and *Eco*RI restriction sites creating plasmid pIADL119 [VanAωC2(L)]. For the larger version of the ω-loop swap of VanA replacing the one of the VanC2 protein [VanC2ωA(L), see Figure 8B], the first round of PCR was conducted as described above using the sense/antisense primer pairs 2099/1bl-A3 and 2bl-A3/1099 and plasmid pIADL121 as template. The resulting PCR-amplified DNA fragments were gel-purified and subjected to a second round of PCR using the 2099/1099 primer pair. The purified SOE-amplified DNA fragment was subcloned into pVanC2 at the *Bam*HI and *Bst*BI restriction sites creating plasmid pIADL122 [VanC2ωA(L)].

Overproduction of His$_6$-Proteins. One colony of freshly transformed *E. coli* strain BL21(DE3) was dispersed in 200 μL of Luria Broth (LB) medium by vortexing, plated onto a kanamycin (50 mg/mL; for plasmids pIADL54, pIADL118, and pIADL119) or ampicilin (100 mg/mL; for plasmids pVanC2, pIADL121 and pIADL122) LB medium agar plate (100 $\times$ 15 mm) and grown overnight at 37 °C. The lawn of cells was resuspended in LB medium (3 mL) and used to inoculate 1 L of LB medium supplemented with 50 mg/mL kanamycin or 100 mg/mL ampicilin. The inoculum was grown at 37 °C to an OD_{600} of 1.0, at which point, isopropyl-1-thio-β-D-galactopyranoside was added to a final concentration of 1 mM. After 4 h of induction at 37 °C or 30 °C, the cells were harvested by centrifugation and used immediately or stored at −80 °C.

Purification of His$_6$-Proteins. All steps were performed at 4 °C unless otherwise noted. Cell pellets from 1 L of culture [expect for K246A VanAωC2(S) for which 3 L was used] were resuspended (2 mL/g of wet cells) in buffer A (50 mM sodium phosphate, pH 8.0, 300 mM NaCl, 10%-(v/v) glycerol, and 2.5 mM imidazole) and disrupted twice in a French pressure cell (18 000 psi). Cellular debris was removed by centrifugation (95000*g*, 20 min), and the supernatant collected was diluted to 20 mL with buffer A. The supernatant was applied to an Ni-NTA superflow column (8 mL, 1.0 mL/min flow rate) previously equilibrated with buffer A, washed with 28 mL of buffer A and then with 150 mL of buffer A containing 20 mM imidazole. The His$_6$-protein eluted with buffer B with a gradient of 20−250 mM imidazole over 50 mL). Fractions (5 mL each) containing the recombinant His$_6$-protein were analyzed for purity by SDS−polyacrylamide gel electrophoresis with the pure fractions pooled. Except for the ω-loop swap proteins and their mutants which were directly aliquoted and frozen as described below, the pooled fractions were dialyzed for two changes, 4 h each, against 2 L of buffer B (50 mM Hepes, pH 7.5, 150 mM KCl and 1 mM EDTA). After dialysis, the protein samples were centrifuged 20 min at 95000*g*, concentrated to 2−8 mg/mL with a Centriprep 30 concentrator (Amicon), aliquoted, and flash frozen in liquid nitrogen for storage at −80 °C. The yield of pure His$_6$-protein obtained from 1 L culture of induced *E. coli* BL21(DE3) cells was ∼20−50 mg, (except for mutants VanAωC2(L)/H320Y/A325R/R251A and VanAωC2(L)/H320Y/A325R/K260A, 5 mg; and mutants VanC2ωA(L)/H320Y/A325R/R251A/K260A and VanAωC2(S)/Y247F, 10 mg).

Protein Quantitation and SDS−Polyacrylamide Gel Electrophoresis. Concentration of pure protein was determined by UV−vis spectroscopy and extinction coefficients [ϵ_{280} = 34 380 $M^{-1}cm^{-1}$ for VanA and VanA mutants except F241Y, ϵ_{280} = 35 870 M^{-1} cm^{-1}; ϵ_{280} = 41 370 M^{-1} cm^{-1} for VanC2 and VanC2 mutants; ϵ_{280} = 35 870 M^{-1} cm^{-1} for VanAωC2-(S) and VanAωC2(S) mutants except Y247F; ϵ_{280} = 34 380 M^{-1} cm^{-1}; ϵ_{280} = 34 380 M^{-1} cm^{-1} for VanAωC2(L); ϵ_{280} = 39 880 M^{-1} cm^{-1} for VanC2ωA(S), VanC2ωA(L), and VanC2ωA(L) mutants except mutants containing the H320Y mutation, ϵ_{280}, 41 370 M^{-1} cm^{-1}] were calculated based on a modification of the Edelhoch method (*27*, *28*). Proteins were separated by SDS−polyacrylamide gel electrophoresis using a discontinuous Tris/glycine buffer (*29*) with 10% acrylamide resolving gels and 5% acrylamide stacking gels containing 0.1% SDS.

Enzyme Assay by Coupled ADP Release. Steady-state kinetic constants for the D-Ala-D-X activities were determined using a spectrophotometric assay monitored at 340 nm where the production of ADP is coupled to the oxidation of NADH through pyruvate kinase and L-lactate dehydrogenase (*30*). The reaction condition 100 mM Hepes, pH 7.5, 10 mM KCl and 10 mM $MgCl_2$ (buffer C), 10 mM ATP, 2.5 mM phosphoenolpyruvate, 0.15−0.2 mM NADH, 50 units/mL L-lactate dehydrogenase, 50 units/mL pyruvate kinase, and D-Ala at 37 °C was used except for the assay performed at multiple pHs (between 6.5 and 8.9) where the 100 mM Hepes was replaced for a composite buffer system containing Mes, Hepes, Tris, and Ches (50 mM each). For assays at pH over 8.20, 100 units/mL pyruvate kinase and L-lactate dehydrogenase were used. For the ω-loop swap proteins (VanAωC2 and VanC2ωA), the assay was performed at 30 °C. Kinetic parameters were determined using the eqs 1−3 previously described (*31*−*34*). To obtain the k_{cat} and K_{M2} values for the D-Ala-D-Ala activities (eq 1), the enzymes were incubated in the above buffer in the presence of increasing concentrations of D-Ala (lowest concentration used 20 mM). K_{M1} was calculated (eq 2) from activity measured at low concentration of D-Ala (0.5−3 mM). The D-Ala-D-lactate activities were measured in the presence of 0.8 mM D-Ala and corrected for the background D-Ala-D-Ala activity. The apparent K_{M2} obtained for D-lactate was corrected using the eq 3 and a K_{M1} for D-Ala of 0.57 mM. All other D-Ala-D-X

activities were measured in the presence of 4 or 10 mM D-Ala and corrected for the background D-Ala-D-Ala activity. The kinetic parameters were determined using the eq 3 and the K_{M1} values from above. For the substrates DL-F-Ala and DL-F_3-Ala, the compounds were considered to be an equimolar mixture of D- and L-isomers, and the L-isomer was assumed to be neither a substrate nor an inhibitor for the enzyme as shown for L-Ala (VLH, IADL and CTW unpublished results).

$$1/v = 1/V_{max} + (K_{M2}/V_{max} \times 1/[S])\, K_{M1} \ll [S] \quad (1)$$

$$[S] \times (1/v - 1/V_{max}) = K_{M2}/V_{max} + [S]K_{M1}K_{M2}/V_{max} \quad (2)$$

$$1/v = 1/V_{max} + K_{M2}/V_{max} \times 1/[S] + K_{M1}K_{M2}/V_{max} \times 1/[S_1] \times 1/[S_2] \quad (3)$$

Coupling Assay by TLC. The ratio of D-Ala-D-Ala to ADP produced by the enzymes was determined using buffer C containing 10 mM α-[^{32}P]ATP (0.5 μCi/mol) and 100 mM D-[^{14}C]Ala (0.3 μCi/μmol) at room temperature. For three time points, the reaction mixtures were analyzed on TLC cellulose plates to separate D-Ala and D-Ala-D-Ala (*8*, *35*) and on TLC cellulose-polyethyleneimine plates to separate ATP and ADP using 0.75 M potassium phosphate, pH 3.5, for development (*36*). The amount of D-Ala-D-Ala and ADP formed was quantified using a phosphoimager (BAS-1000 Fujix) and corrected for nonenzymatic activity. The ratio of D-Ala-D-hydroxybutyrate to ADP produced was determined as above using α-[^{32}P]ATP (0.05 μCi/mol), 0.5 mM D-[^{14}C]-Ala (55 μCi/μmol), and 100 mM DL-hydroxybutyrate.

Separation of D-Ala-D-F_x-Ala by TLC. For production of D-Ala-D-F_x-Ala, 100 mM Mes, pH 6.0, 10 mM KCl, 10 mM $MgCl_2$, 10 mM ATP, 0.5 mM D-[^{14}C]Ala (0.3 μCi/μmol), and either 50 mM DL-F_3-Ala, 25 mM D-F_2-Ala, or 50 mM DL-F_1-Ala were incubated with VanA at room temperature for 1 h. D-Ala-D-Ala was formed similarly using Hepes, pH 8.0, or Mes, pH 6.0, buffer without D-F_x-Ala present. The reaction mixtures were analyzed on TLC silica plates to separate D-Ala, D-Ala-D-Ala, and D-Ala-D-F_x-Ala using 25% 1 M ammonium acetate in 2-propanol for development (*37*). The D-[^{14}C]Ala containing spots were visualized using a phosphoimager. The R_f values for D-Ala, D-Ala-D-F_1-Ala, D-Ala-D-F_2-Ala, and D-Ala-D-F_3-Ala were 0.23, 0.26, 0.38, and 0.50, respectively. D-Ala-D-Ala migrated less than D-Ala, but overlapped the D-Ala spot.

RESULTS

pH Profile Study of D-Ala-D-Ala Activity of VanA. The D-Ala-D-lactate ligases, unlike the D-Ala-D-Ala and D-Ala-D-Ser ligases, can catalyze the formation of both the ester (D-Ala-D-lactate) and peptide linkage (D-Ala-D-Ala or D-Ala-D-Ser). For VanA, the catalysis of ester formation is strongly favored over peptide formation, despite the 17-fold greater turnover number for peptide (k_{cat} of 550 min^{-1}) vs depsipeptide (k_{cat} of 32 min^{-1}) formation (Table 4). This selectivity in catalysis at physiological pH (~7.5) is ensured by a ~300-fold higher affinity of VanA for D-lactate (K_{M2} of 0.69 mM) compared to D-Ala_2 (K_{M2} of 210 mM). Similar kinetics for peptide and ester linkage formation is also observed for the LmDdl2 D-Ala-D-lactate ligase (*17*). Thus, to achieve catalysis of their physiological ester product, the D-Ala-D-lactate ligases have evolved a differential mechanism that allows preferential recognition of the α-hydroxyl of D-lactate over the α-ammonium of D-Ala at subsite 2. Two distinctions between D-lactate and D-Ala are the pK_a values of the ionizable α-hydroxyl (~14) and α-ammonium (9.87) groups and the different charge states of the predominant species in the pH range 6−9 (lactate a monoanion, D-Ala a zwitterion) where the depsipeptide and dipeptide activities of D-Ala-D-X ligases are measured (*38*). We have previously shown that the catalytic efficiency of VanA for D-Ala-D-Ala but not D-Ala-D-lactate formation is dependent on pH (*39*). This pH dependence is much more pronounced in the case of VanA than DdlB (*39*). We have here extended the study of the VanA kinetics for D-Ala-D-Ala formation at various pHs.

Table 2 reveals that the catalytic efficiency (k_{cat}/K_{M2}) for D-Ala-D-Ala production increased by 22-fold over a span of 1.55 pH units (from 7.25 to 8.80). We did not evaluate the K_{M1} values for D-Ala_1 at the various pHs in this study, since previous work has shown that the K_{M1} values remain unchanged within the pH range of 7.5−9.2 (*39*). The k_{cat} values were constant within the pH range examined. This result is in contrast to that for DdlB where the k_{cat} values increased and D-Ala_2 K_{M2} values decreased slightly with increasing pH (*39*). Therefore, the effect of the pH on the catalytic activity of VanA is reflected in a change in K_{M2} values only (27-fold from pH 7.25 to 8.80) (Figure 4A and Table 2).

A plot of the log of ($1/K_{M2}$) vs pH when compared with the log of the mole fraction of the free amine of D-Ala vs pH indicates a direct dependence of the K_{M2} values on the mole fraction of free amine present in solution (Figure 4B) and suggests that the deprotonated (NH_2) form of D-Ala is predominantly (perhaps exclusively) recognized at subsite 2 of VanA and subject to catalysis. With the assumption that only the free base form of D-Ala_2 binds productively, correction of the overall D-Ala concentration for the concentration of its free amine form at the various pHs revealed K_{M2} values that are pH independent in the pH range 7.25−8.80 (varies between 0.55 and 0.89 mM, average of 0.66 mM, Table 2). One might argue that amino acid side chains titrating within the pH range examined may also contribute to the change in the observed K_{M2} values; however, D-lactate and D-F_3-Ala (see section below), whose α-hydroxyl and α-ammonium, respectively, do not change charge states in the pH range examined show pH independent (pH 7.5−8.5) K_{M2} values (Table 2) (*39*). These results suggest that a putative change in the protonation state of the active site of VanA does not significantly affect the binding of the uncharged 2-NH_2 and 2-OH forms of D-Ala and D-lactate.

pH-Rate Profile of D-Ala-D-F_x-Ala Activity of VanA Using Fluorinated D-Ala Derivatives as Substrates for Subsite 2. Given the differential recognition and processing of the monoanionic D-lactate versus zwitterionic D-Ala_2 by VanA, we turned to D-Ala analogues with a markedly lower pK_a to evaluate catalytic efficiency when a higher mole fraction of the uncharged amino group is present at pHs between 6.5 and 8.5: D-F-Ala (pK_a, 8.35), D-F_2-Ala (pK_a, 7.25), and D-F_3-Ala (pK_a, 5.85) (*40*). When tested as a substitute for both D-Ala_1 and D-Ala_2, D-F_3-Ala and D-F_2-Ala were very poor substrates, and D-F-Ala was a slightly better substrate (data not shown). On the other hand, if enough D-Ala is added to saturate the high affinity (K_{M1}, 0.57 mM) D-Ala_1 site, then

Table 2: Kinetic Parameters of VanA at Various pH for D-Ala and Fluorinated Derivative of D-Ala[a]

substrate	pH	K_{M2}[b] (mM)	k_{cat} (min^{-1})	k_{cat}/K_{M2} (min^{-1}/mM)	Fraction of amine[c]	K_{M2} corrected (mM)[d]	K_{M2} corrected average (mM)
D-Ala	7.25	270	610	2.3	0.0024	0.65	
	7.50	210	550	2.6	0.0043	0.89	
	7.70	82	540	6.6	0.0067	0.55	
	7.90	61	530	8.7	0.0106	0.65	
	8.15	30	510	17	0.0187	0.56	
	8.35	20	500	25	0.0293	0.59	
	8.55	14	510	36	0.0510	0.71	
	8.80	10	480	51	0.0872	0.87	0.66
D-F-Ala[e,f]	6.45	160	620	3.9	0.012	2.0	
	6.85	69	580	8.4	0.031	2.1	
	7.30	26	510	19	0.082	2.1	
	7.50	20	490	25	0.124	2.5	
	7.55	16	480	30	0.137	2.2	
	7.80	9.6	470	49	0.220	2.1	
	8.00	7.2	470	65	0.309	2.2	
	8.30	4.6	440	96	0.471	2.2	
	8.50	3.9	410	110	0.586	2.3	2.2
D-F_2-Ala[f]	6.50	21	470	22	0.151	3.2	
	7.00	7.0	485	69	0.360	2.5	
	7.50	4.0	600	150	0.640	2.6	
	8.05	3.4	635	180	0.863	2.9	
	8.50	3.3	450	140	0.947	3.1	2.9
D-F_3-Ala[e,f]	6.00	17	530	32	0.817	14	
	7.05	13	520	40	0.941	12	
	7.50	12	510	43	0.978	12	
	8.00	12	510	43	0.993	12	
	8.50	13	440	39	0.998	13	12

[a] Measured by ADP coupled assay (see Materials and Methods). [b] K_M at subsite 2 [K_M for D-Ala at subsite 1 does not change significantly (*39*)]. [c] Molar fraction of the free amine form of the substrate at a given pH [calculated based on pK_a: 9.87 (D-Ala), 8.35 (D-F-Ala), 7.25 (D-F_2-Ala), and 5.85 (D-F_3-Ala) (*40*)]. [d] K_M corrected for the concentration of the free amine form of the substrate at a given pH. [e] Mixture of D- and L-enantiomer, assumed to be an equimolar ratio; L-Ala is not a substrate nor a inhibitor (result not shown). [f] A concentration of 4 mM D-Ala were used to saturated the subsite 1.

the rate of coupled ATP hydrolysis increases for all the fluorinated D-Ala substrates (Table 2) as D-Ala-D-F_x-Ala (x = 1, 2, and 3) is produced. Separation of the reaction mixtures by TLC using D-[^{14}C]Ala revealed new radioactive spots that were only formed in the presence of D-F_x-Ala and migrated faster than [^{14}C]D-Ala-D-Ala confirming that the expected D-Ala-D-F_x-Ala products are formed (Figure 5).

When D-F-Ala was used as a substitute for D-Ala_2, the catalytic efficiency (k_{cat}/K_{M2}) remained dependent on the pH but in a less pronounced manner than for D-Ala (Table 2), and at pH 7.5 the K_{M2} values were 210 mM for D-Ala_2 versus 20 mM for D-F-Ala. The pH dependency of the catalytic efficiency was even further diminished when D-F_2-Ala was used as a substitute for D-Ala_2 (K_M D-F_2-Ala of 4 mM at pH 7.5) and almost absent for D-F_3-Ala from pH 6.5 to 8.5. Similar to that for D-Ala-D-Ala activity, the changes in catalytic efficiency with pH in the mono/di/trifluoroalanine series were due to changes in K_{M2}, not k_{cat} (Table 2 and Figure 6A). For all three fluorinated D-Ala analogues, the change in the observed K_{M2} again parallels the mole fraction of the free amine as calculated from their respective pK_as and is consistent with VanA using only the free base form of the substrate at subsite 2 for catalysis (Table 2 and Figure 6B). Correction of the fluorinated D-Ala concentration for the concentration of its free amine form in solution reveals a K_{M2} of 2.2 mM for D-F-Ala, 2.9 mM for D-F_2-Ala, and 12 mM for D-F_3-Ala, all of which are pH independent. Given invariant k_{cat} values for all the fluorinated analogues and D-Ala over a range of 4 pK_a units, it would appear that the reduction in the nucleophilicity of the amine group by the fluorine atoms is not significant enough for nucleophilic attack on the activated D-alanyl phosphate intermediate to become rate limiting (Scheme 1).

pH Profile Study of D-Ala-D-Ala Activity of LmDdl2. The D-Ala-D-Ala activity of LmDdl2, a representative of the other D-Ala-D-lactate ligase subfamily (Figure 3), was also analyzed at various pH values to see if a similar mechanism of charge rejection of the protonated form of D-Ala_2 was used to favor D-Ala-D-lactate synthesis. However, when D-Ala-D-Ala activity was assayed, it was not possible to approach saturation in order to obtain K_{M2} values even at pHs as high as 8.5, and data collection was complicated by an observed increase in the K_{M1} value for D-Ala_1 with pH (data not shown). When D-F_3-Ala was tested as a substitute for D-Ala_2 to see if the enzyme prefers the free amine form of D-amino $acid_2$, again saturation was not reached so K_{M2} values could not be determined (data not shown). Although, the possibility that the fluorine atoms significantly increase the K_{M2} of D-F_3-Ala cannot be excluded, LmDdl2 seems to bind poorly both the deprotonated and protonated forms of D-Ala_2.

pH Profile of VanA for D-Ala-D-X Dipeptide Formation. We have previously shown that VanA prefers D-amino acids with larger side chains than the methyl group of D-Ala at subsite 2 (*35*). However, these determinations were performed at only one pH, and this apparent preference could be partially due to the difference in the pK_a of the amines of the different amino acids. When the D-amino acid D-Ser (pK_a of the amine group, 9.15) was evaluated as substitute for D-Ala_2 (pK_a, 9.87) for dipeptide formation at various pHs,

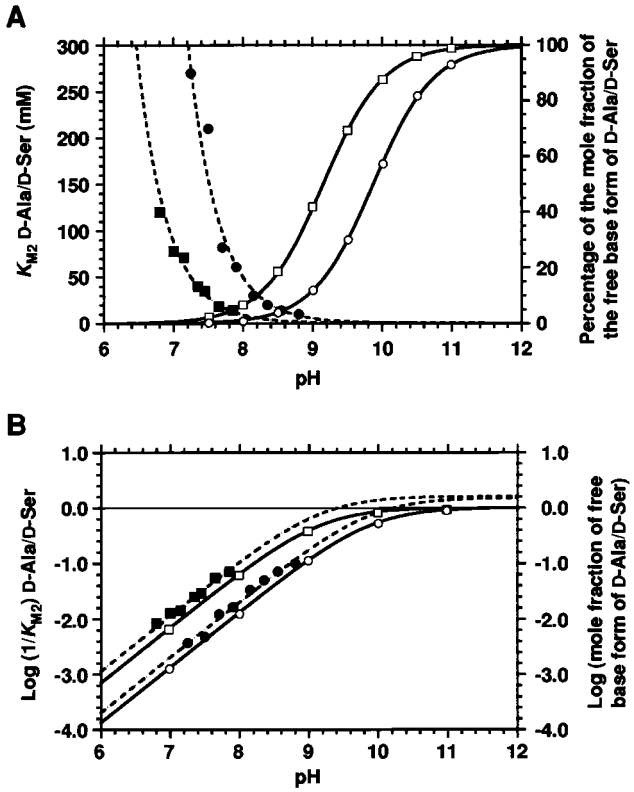

FIGURE 4: pH profile of D-Ala and D-Ser K_{M2} values for VanA. (A) D-Ala K_{M2} values (dashed line and closed circles), D-Ser K_{M2} values (dashed line and closed squares) and percent of the mole fraction of free amine for D-Ala (solid line and open circles) and D-Ser (solid line and open squares) as a function of pH. (B) Direct correlation of log of $1/K_{M2}$ for D-Ala and D-Ser with the log of the mole fraction of free amine for D-Ala and D-Ser.

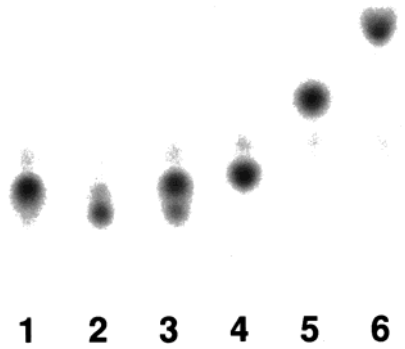

FIGURE 5: TLC of D-Ala-D-F_x-Ala products formed by VanA. Lane 1, D-[^{14}C]Ala standard. Lane 2, D-[^{14}C]Ala incubated with VanA at pH 8.0 to form D-Ala-D-Ala. Lane 3, same as lane 2 except at pH 6.0. Lanes 4−6, VanA incubated at pH 6.0 with D-[^{14}C]Ala and either DL-F_1-Ala (lane 4), D-F_2-Ala (lane 5), or DL-F_3-Ala (lane 6) to form the respective D-Ala-D-F_x-Ala products. TLC conditions as described in Materials and Methods.

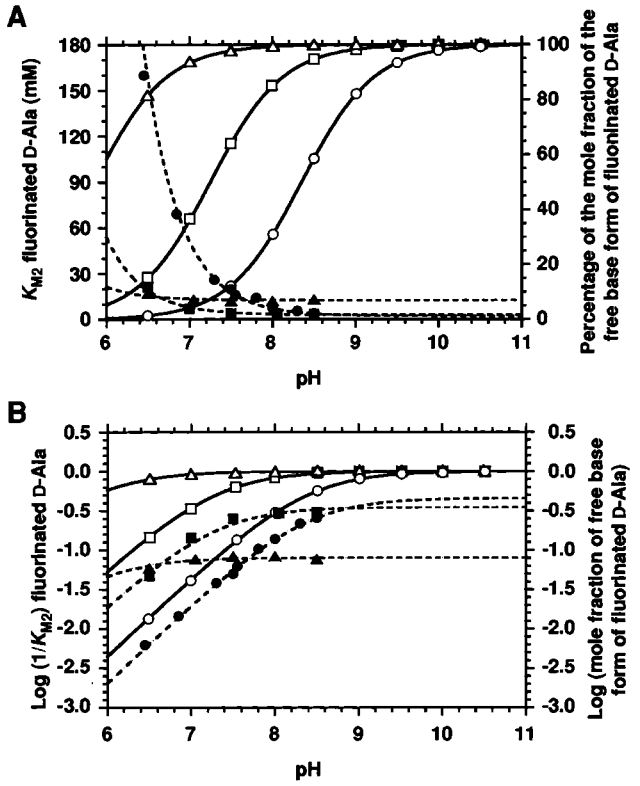

FIGURE 6: pH profile of fluorinated D-Ala K_{M2} values for VanA. (A) Fluorinated D-Ala K_{M2} values (dashed lines and closed symbols) and percent of the mole fraction of free amine substrate (solid lines and open symbols) as a function of pH. Circles, D-F-Ala; squares, D-F_2-Ala; triangles, D-F_3-Ala. (B) Direct correlation of log of $1/K_{M2}$ (dashed lines) with the log of the mole fraction of free amine substrate (solid lines).

Scheme 1

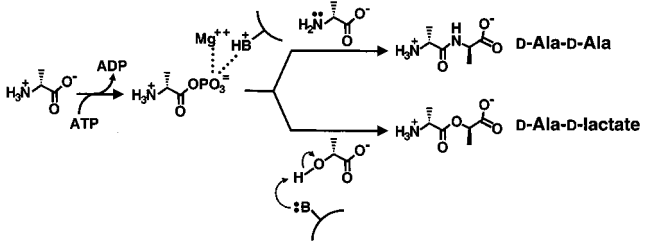

the decrease of K_{M2} again correlated with the increase of pH and the fraction of the deprotonated form, suggesting that the protonated form is also rejected at the subsite 2 (Table 3 and Figure 4). Interestingly, the predicted K_{M2} for the deprotonated form of D-Ser (0.62 mM) is similar to that of D-Ala (0.66 mM). For example, at pH ~7.5, the apparent ~5-fold lower K_{M2} of D-Ser vs D-Ala can be ascribed to the commensurately higher mole faction of the D-Ser free amine at this pH. Thus, VanA is equally capable of binding the free amine forms of D-Ala_2 and D-Ser. This is in contrast to DdlB, which has a 20-fold preference for D-Ala-D-Ala synthesis over D-Ala-D-Ser synthesis (*32*). This result may be in accord with the dendrogram in Figure 3. The closest related subfamily to VanA is the VanC subfamily, likely to have evolved from a common ancestor. Furthermore, the residues just outside of the putative ω-loop are very similar (see below, and Figure 1D and 8B) and one of the determinants for D-Ser recognition by VanC2 shown to be Arg322 (*37*) is also conserved in the VanA subfamily. When the corresponding conserved arginine residue in VanA (Arg317) was mutated to methionine, the catalytic efficiency dropped drastically for all D-Ala-D-X activities, indicating that this residue is indeed crucial in maintaining the active site (Table 4).

Since VanA appears to bind the deprotonated from of D-Ala_2 and D-Ser with equal affinity as well as the α-hydroxy acid cognate of D-Ala, D-lactate, the α-hydroxy acid cognate of D-Ser, D-glyceric acid, was tested as a substrate. However, no D-Ala-D-glyceric acid depsipeptide formation was detectable by either TLC or ADP coupled assay.

Table 3: Kinetic Parameters of VanA at Various pH for D-Ser[a]

substrate	pH	K_{M2}[b] (mM)	k_{cat} (min^{-1})	k_{cat}/K_{M2} (min^{-1}/mM)	fraction of amine[c]	K_{M2} corrected (mM)[d]	K_{M2} corrected average (mM)
D-Ser[f]	6.80	120	71	0.59	0.0044	0.53	
	7.00	78	78	1.02	0.0070	0.55	
	7.15	71	139	2.0	0.0099	0.70	
	7.35	40	80	2.0	0.0156	0.62	
	7.45	35	160	4.6	0.0196	0.69	
	7.65	18	73	4.1	0.0307	0.56	
	7.85	14	147	11	0.0477	0.67	0.62

[a] Measured by ADP coupled assay (see Materials and Methods). [b] K_M at subsite 2 [K_M for D-Ala at subsite 1 does not change significantly (*39*)]. [c] Molar fraction of the free amine form of the substrate at a given pH [calculated based on pK_a of 9.15 (*38*)]. [d] K_M corrected for the concentration of the free amine form of the substrate at a given pH. [e] Mixture of D- and L-enantiomer, assume an equimolar ratio; L-isomer is not a substrate nor a inhibitor (result not shown). [f] A concentration of 4 mM D-Ala were used to saturated the subsite 1.

Table 4: Kinetic Parameters of VanA Mutant Proteins for D-Ala-D-Ala and D-Ala-D-lactate Formation[a]

	D-Ala-D-Ala formation				D-Ala-D-lactate formation		
protein	K_{M1}[b] (mM)	K_{M2}[c] (mM)	k_{cat} (min^{-1})	k_{cat}/K_{M2} (min^{-1} mM^{-1})	K_M (mM)	k_{cat} (min^{-1})	k_{cat}/K_M (min^{-1} mM^{-1})
VanA	0.40	160	500	3.1	0.69	35	51
His-VanA[d]	0.57	210	550	2.6	0.68	32	47
His-K50A	0.75	170	490	2.9	0.81	31	38
His-C52A	0.88	175	480	2.7	0.66	29	44
His-E60A	0.82	165	380	2.3	0.53	27	51
His-S70A	1.0	200	370	1.9	0.64	19	30
His-D72A	70	nd[e]	nd	0.047	nd	nd	nd
His-H76A	0.76	155	300	1.9	0.79	21	27
His-E230A	1.0	125	430	3.4	0.68	30	44
His-D232A	0.82	nd	nd	0.049	nd	nd	0.0062
His-Q233A	2.0	300	520	1.7	0.51	23	45
His-F241A	2.1	nd	nd	0.49	*f*		
His-F241Y	1.1	210	460	2.2	1.7	36	21
His-R242A	1.2	62	530	8.5	0.69	27	39
His-H244A	1.4	87	540	6.2	53	16	0.30
His-R242A/H244A	0.66	69	580	8.4	60	12	0.20
His-Q245A	1.6	270	580	2.1	6.3	30	4.8
His-E246A	1.9	160	490	3.1	5.5	34	6.2
His-P249A	1.5	220	660	3.0	2.8	44	16
His-E250A	1.3	160	550	3.4	1.1	35	32
His-K251A	0.87	230	610	2.7	1.7	38	22
His-S253A	1.3	130	490	3.8	1.6	41	25
His-E254A	1.1	150	520	3.5	0.70	36	51
His-N255A	3.4	290	510	1.8	2.7	40	15
His-R317M	>200[g]	nd	nd	0.016	nd	nd	nd

[a] Measured by ADP coupled assay at pH 7.5 (Materials and Methods). [b] K_M at subsite 1. [c] K_M at subsite 2. [d] His_6-tagged VanA protein. [e] Not detectable/determined. [f] Not measured. [g] Highest concentration tested.

Selection and Production of VanA Mutants. In addition to the divergence of primary sequence of the VanA and VanB Ddl family from the other four Ddl families in the ω-loop region, there was also a difference at the N-terminus, an insertion of approximately 33 residues that led us to examine that region as well as the 26 residue stretch from 230 to 255 in the putative ω-loop region of the VanA enzyme (Figure 1, panels B and D). To facilitate purification of the VanA mutants, all were expressed as His_6-tagged proteins, allowing single-step affinity purification after overproduction in the *E. coli* host strain. The kinetic parameters measured for purified wild-type His_6−VanA enzyme were identical to VanA without the His_6-tag at the N-terminus (Table 4), so all the kinetic parameters listed in Table 4 are for the mutant proteins as His_6−VanA fusions.

When VanA and VanB ligases are compared and mapped onto the X-ray structure of *E. coli* DdlB as a predictive model (Swen G. Hyberts, personal communication) using the program consensus (*41*), there is a 38 residue insert, Cys50−Glu87, that is not present in DdlB. Efforts to overproduce a VanB protein with those 38 residues deleted gave only insoluble protein so the hypothesis that these residues are not essential for catalytic activity could not be tested (I.A.D.L. and C.T.W. unpublished results). When six conserved residues (VanA superfamily) in this region of VanA, Lys50, Cys52, Glu60, Ser70, Asp72, and His76 were singly mutated to alanine, five were without effect. The D72A mutant had almost a 200-fold increase in K_{M1} for D-Ala and a corresponding loss in catalytic efficiency (k_{cat}/K_M). The basis of this defect is not yet understood.

Of the 26 residues in VanA encompassing sequence that is predicted to lead into, include, and lead out of a loop (Figure 1D) corresponding to the crucial ω-loop of Ddls, 14 were selected for mutagenesis to alanine as listed in Table 4. The basis for selection was either any side chain with a functional group (aspartate, glutamate, histidine, lysine, arginine, and serine) or a phenylalanine, or a glutamine, asparagine, or proline because of possible hydrogen-bonding or structure-disrupting effects. All 14 mutants were obtained in pure form and evaluated for catalytic efficiencies compared

Table 5: Kinetic Parameters of VanA Mutant Proteins at Various pH for D-Ala[a]

protein	pH	K_{M2}[b] (mM)	k_{cat} (min^{-1})	k_{cat}/K_{M2} (min^{-1}/mM)	fraction of amine[c]	K_{M2} corrected (mM)[d]	K_{M2} corrected average (mM)
His-R242A	6.90	180	570	3.2	0.0011		
	7.15	120	590	4.9	0.0019		
	7.40	72	520	7.2	0.0034		
	7.50	62	530	8.5	0.0043		
	7.65	44	540	12	0.0060		
	7.80	36	500	14	0.0084		
	8.00	26	540	20	0.0133		
	8.25	20	510	26	0.0234		
	8.40	14	510	36	0.0328		
	8.60	10	500	50	0.0510	na[f]	na
His-H244A	7.00	260	630	2.4	0.0013		
	7.25	160	630	3.9	0.0024		
	7.40	100	620	6.2	0.0034		
	7.50	84	600	7.1	0.0043		
	7.60	81	640	7.9	0.0053		
	7.75	54	650	12	0.0084		
	8.00	37	640	17	0.0133		
	8.15	26	640	25	0.0187		
	8.35	20	660	33	0.0293		
	8.60	12	640	53	0.0510	na	na
His-H244A/R242A	7.00	190	590	3.1	0.0013		
	7.25	110	550	5.0	0.0024		
	7.40	87	550	7.2	0.0034		
	7.50	69	580	8.4	0.0043		
	7.65	51	560	11	0.0060		
	7.75	48	570	12	0.0084		
	8.00	28	590	21	0.0133		
	8.20	19	560	29	0.0209		
	8.40	16	570	36	0.0328	na	na
His-K251A	7.25	240	610	2.5	0.0024	0.58	
	7.50	230	610	2.7	0.0043	0.99	
	7.75	75	610	8.1	0.0084	0.63	0.67
	8.00	45	450	10	0.0133	0.60	
	8.15	33	510	15	0.0187	0.62	
	8.35	21	500	24	0.0293	0.62	
	8.60	13	580	45	0.0510	0.66	
	8.85	7.9	610	77	0.0872	0.69	

[a] Measured by ADP coupled assay (see Materials and Methods). [b] K_M at subsite 2 [K_M for D-Ala at subsite 1 does not change significantly (*39*)]. [c] Molar fraction of the free amine form of the substrate at a given pH [calculated based on pK_a of 9.87 (D-Ala) (*38*)]. [d] K_M corrected for the concentration of the free amine form of the substrate at a given pH. [e] Mixture of D- and L-enantiomer, assumed to be an equimolar ratio; L-Ala is not a substrate nor a inhibitor (result not shown). [f] Not applicable.

to wild-type, both for D-Ala-D-Ala dipeptide and D-Ala-D-lactate depsipeptide ligase activity.

Only two of the 14 mutations affected dipeptide ligase activity, consistent with the expectation that this is a largely unstructured region of the enzyme. The two mutations that alter k_{cat}/K_{M2} are F241A and D232A. The F241A is lowered only 6-fold. In a follow on F241A, the dipeptide catalytic efficiency of F241Y is back within wild-type VanA levels and the depsipeptide ligase catalytic efficiency remains the same as wild-type VanA. Thus, Phe241 is not comparable to F261Y in the LmDdl2 ω-loop (*17*). The D232A mutant is more substantially disabled, with a 60-fold decline in catalytic efficiency at pH 7.5. When D232A VanA was assessed for D-Ala-D-lactate ligase activity, it was dramatically less efficient still: indeed with a 10000-fold drop in k_{cat}/K_{M2}, the depsipeptide ligase is affected about 2 orders of magnitude more than the dipeptide ligase activity of the same active site. To see if Asp232 was a determinant for selection/catalysis between D-Ala_2 and D-lactate, we tested D-Ala-D-Ala activity assayed at a higher pH (8.55) where a greater percentage of free amine is present (~5%) and also D-Ala-D-F_3-Ala formation at pH 7.5 (~97% free base form). The D-Ala-D-Ala activity was down by 300-fold, while the D-Ala-D-F_3-Ala was down by 3000-fold compared to wild-type, suggesting Asp232 is not a specific determinant for D-Ala-D-lactate activity. The Asp232 residue and the residues just around it are also highly conserved in the VanC subfamily, the closest homologue to the VanA subfamily, but not in other subfamiles (see below and Figures 1D and 8B). To explore the role of this residue further, the corresponding D241A mutation was also made in VanC2. When tested as a D-Ala-D-Ser ligase, D241A VanC2 had a 66-fold lower k_{cat} and a 210-fold higher D-Ser K_{M2} than wild-type VanC2 for a 14000-fold decrement in catalytic efficiency (Table 6). On the other hand, the catalytic efficiency of D-Ala-D-Ala formation was only down by 18-fold. This aspartate mutation in both VanA and VanC2 has a greater effect on the catalytic efficiency for the specific second substrate, D-lactate or D-Ser.

Two comments about the D-Ala-D-Ala ligase activity of the K251A and H244A mutants: first, these two residues, along with Arg242, are the only residues in this stretch with basic side chains that could stabilize phosphoryl transfer, and there was no alteration of dipeptide ligase activity at pH 7.5

Table 6: Kinetic Parameters of VanA and VanC2 ω-Loop Swap Proteins for D-Ala-D-Ala and D-Ala-D-Ser Formation[a]

	D-Ala-D-Ala formation			D-Ala-D-Ser formation		
protein[c]	K_{M2}[b] (mM)	k_{cat} (min^{-1})	k_{cat}/K_{M2} (min^{-1} mM^{-1})	K_{M2} (mM)	k_{cat} (min^{-1})	k_{cat}/K_M (min^{-1} mM^{-1})
VanA	220	230	1.0	34	100	3.0
VanAωC2(S)	34	100	3.0	6.3	38	5.9
VanAωC2(L)	42	9.6	0.23	5.6	1.8	0.32
VanAωC2(S).K246A	480	87	0.18	78	35	0.45
VanAωC2(S).Y247F	213	74	0.35	21	40	1.9
VanC2	>100[d]	>44[e]	0.36	1.0	210	210
VanC2.K255A	nd[f]	nd	nd	16	0.56	0.036
VanC2.D241A	>200[d]	>3.5[e]	0.020	210	3.2	0.015
VanC2ωA(S)	>200[d]	>0.92[e]	0.045	>200[d]	>0.84[e]	0.0044
VanC2ωA(L)	nd	nd	nd	nd	nd	nd
VanC2ωA(L)[g]	>170[d]	>3.3[e]	0.019	3.1	3.7	1.2
VanC2ωA(L).K260A[g]	nd	nd	nd	nd	nd	nd
VanC2ωA(L).R251A[g]	nd	nd	nd	nd	nd	nd
VanC2ωA(L).K260A.R251A[g]	nd	nd	nd	nd	nd	nd

[a] Measured by ADP coupled assay at pH 7.5 (Materials and Methods). [b] K_M at subsite 2. [c] His_6-tagged proteins. [d] Highest concentration tested. [e] Activity at highest concentration tested. [f] Not detectable. [g] Contain mutations H320Y and A325R.

on mutation to alanine nor did mutation of K50A or H76A have any effect. Second, the H244A and R242A mutants are, if anything, perhaps 2−3-fold better as a dipeptide ligase at pH 7.5 than wild-type VanA by k_{cat}/K_{M2} criterion due to a lower K_{M2} for D-Ala_2 (see below). This is in substantial contrast to the catalytic efficiency of H244A but not the R242A mutant as a D-Ala-D-lactate depsipeptide ligase. In several independent preparations, the depsipeptide ligase activity (k_{cat}/K_{M2}) of H244A VanA was selectively disabled by 150-fold, predominantly due to a 2 orders of magnitude worsening of the K_M for D-lactate. The ratio of depsipeptide/dipeptide ligase activity of H244A VanA compared to the same catalytic efficiency ratio in wild-type VanA is down by 300-fold. Alanine scanning of residues immediately downstream of His244, Gln245, and Glu246 gave noticeable but smaller selective effects on the catalytic efficiency for depsipeptide ligation of 10−12-fold and 8-fold, respectively, as though some misorientation in this region had a secondary effect on the placement/orientation of His244.

Coupling of ATPase to Dipeptide/Depsipeptide Ligase Activity. The ω-loop and N-terminal VanA mutants were tested to see if ADP formation was coupled one for one to dipeptide and depsipeptide formation. In the mechanistically and structurally cognate glutathione synthetase, when a loop that closes over the active was replaced with a short peptide composed of four glycine residues, the amount of the reactive γ-L-glutamyl-L-cysteinyl phosphate intermediate hydrolyzed by water increased to two-thirds (*42*). Similarly, another member of the ATP grasp superfamily, PurT Gar Transformylase, was found to release formyl phosphate when a residue in its ω-loop was mutated giving G162I (*43*). Thus, we were hoping to find an uncoupled mutant that produced D-alanyl phosphate but did not proceed to form product to prove the formation of this putative enzyme intermediate. The ratio of α-[^{32}P]ADP to [^{14}C]D-Ala-D-Ala or [^{14}C]D-Ala-D-hydroxybutyrate produced was determined by analyzing the reaction mixtures using separate TLC systems to quantitate the ATP converted to ADP and the D-Ala converted to dipeptide or depsipeptide. Wild-type VanA, VanC2, and DdlB enzymes were fully coupled with one ADP formed per dipeptide or depsipeptide. All the VanA mutants were also coupled except for D232A VanA. This mutant was coupled for D-Ala-D-Ala activity but only about 10−20% coupled for D-Ala-D-hydroxybutyrate activity. However, attempts to trap enzyme bound or released D-alanyl phosphate with hydroxylamine to form the stable D-Ala hydroxamate were unsuccessful. It is possible that D-Ala-D-hydroxybutyrate formation is sufficiently impaired that an active-site water molecule competes with hydroxybutyrate for D-alanyl phosphate capture.

pH Profile for D-Ala-D-Ala Activity for the VanA Mutants R242A, H244A, K251A, and R242A/H244A. As shown above, VanA rejects the protonated form of D-Ala_2 as a mechanism to ensure efficient formation of D-Ala-D-lactate compared to D-Ala-D-Ala at physiological conditions. In contrast, DdlB accepts the protonated form of D-Ala_2 (*39*, *44*) and since most of the active site is conserved among the Ddl families including the VanA subfamily (Figure 2), we investigated the possible role of residues with positively charged side chains in rejecting the protonated form of D-Ala_2, in and around the putative corresponding ω-loop region of VanA (Figure 1D).

The pH profile of the K251A mutant was found to be identical to that of the wild-type VanA, indicating that the protonated form of D-Ala_2 is still efficiently rejected at the active site (Table 5 and Figure 7). The calculated K_{M2} value for the deprotonated form (NH_2) of D-Ala_2 is 0.67 mM, which is identical to the wild-type (0.66 mM). After the experiment was completed, two other D-Ala-D-lactate ligases from vancomycin-type producer organisms (DdlN and DdlM) were cloned and sequenced and revealed a threonine residue instead of a lysine residue at this locus (*45*) further suggesting that it is not a crucial residue. On the other hand, the R242A mutant clearly reveals an altered pH profile (Table 5 and Figure 7). While the k_{cat} remains unchanged with pH, the observed decrease in K_{M2} for D-Ala with an increase in pH was about 2−4-fold less than for the wild-type enzyme or K251A VanA (K_{M2} at pH 7.5 = 62 mM vs 230 mM for wild-type VanA), suggesting a lessened discrimination against the use of the protonated form of D-Ala as a substrate. Noticeably, the DdlN and DdlM ligases present a lysine residue in place of the arginine residue, a conservative mutation consistent with the importance of the positive charge at this position for rejecting the charged amino acid at the subsite 2. The H244A mutant is distinct from wild-

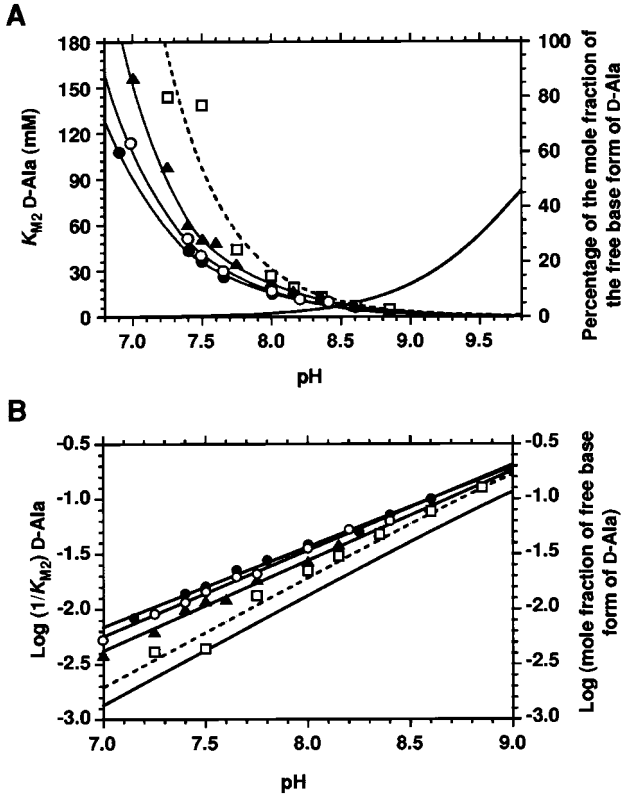

FIGURE 7: pH profile of D-Ala-D-Ala activity by VanA mutants. (A) D-Ala K_{M2} values (lines with symbols) and percent of the mole fraction of free amine substrate (solid line without symbols) as a function of pH. Squares, K251A VanA; triangles, H244A VanA; open circles, R242A/H244A VanA; closed circles R242A VanA. (B) Direct correlation of log of $1/K_{M2}$ for wild-type and K215A VanA with the log of the mole fraction of free amine substrate (solid line without symbols).

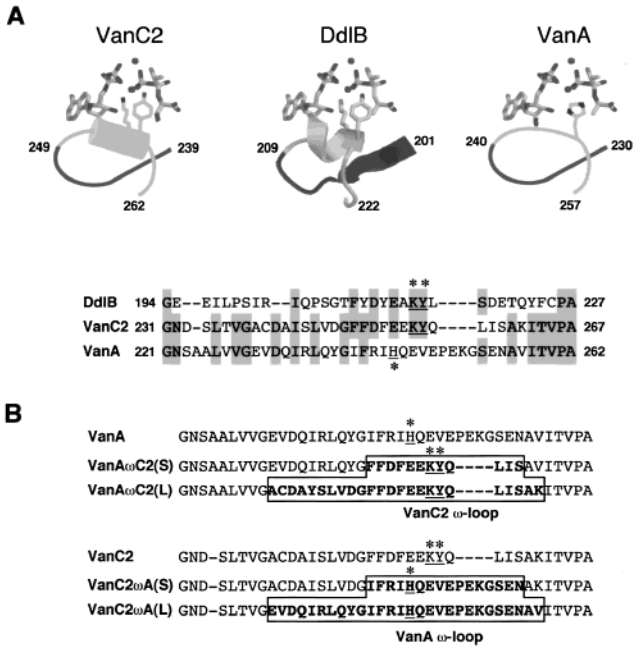

FIGURE 8: Strategy for ω-loop swap mutants. (A) Schematic view of the putative ω-loops of VanA and VanC2 based on the structure of DdlB (*20*) and the corresponding primary sequence of the putative loops. Highlighted residues are identical in at least two of the enzymes. Lys215 and Tyr216 which are important for activity in DdlB and VanC2 are starred and underlined. His244, crucial for D-Ala-D-lactate activity in VanA, is also starred and underlined. (B) Sequence of the residues in and adjacent to the putative VanA ω-loop and the sequence of two swap mutants with the portions of the VanC2 ω-loop inserted into VanA in bold. The primary sequence in and adjacent to the VanC2 ω-loop is also listed followed by the sequence of swap mutants with the portion of the putative VanA ω-loop inserted into VanC2 in bold. Lys255 and Tyr256 in the VanC2 ω-loop and His244 in the putative VanA ω-loop are underlined and starred.

type VanA but does have a steeper slope in log $1/K_{M2}$ vs pH than R242A (Figure 7B). The double mutant R242A/H244A VanA shows properties equivalent to the R242A single mutant, with about half the slope in the log $1/K_{M2}$ vs pH plots of wild-type VanA. Thus, the cationic side chain of R242A may contribute but is not the sole determinant of discrimination against the D-Ala$_2$ zwitterion. Given that the K_{M2} for the free base form of D-Ala$_2$ in H244A extrapolates to less than or equal to 5 mM (<8-fold over the 0.66 mM value in wild-type VanA) while the D-lactate K_{M2} is up 100-fold over wild-type VanA, His244 is a specific determinant for recognition of D-lactate.

ω-Loop Swapping between VanA and VanC2. Because of the importance of amino acids in the ω-loop for catalysis by each family of D-Ala-D-X ligases (histidine and arginine in the VanA subfamily, and lysine and tyrosine/phenylalanine in all the others) and because of the striking difference between the proposed ω-loop of VanA to that of the other family members, we attempted to establish whether the ω-loops are necessary and sufficient to determine the activity profile of each ligase. We chose to swap the ω-loops of VanC2 and VanA because the primary sequence just upstream and downstream of the ω-loop of the VanA subfamily is more homologous to the VanC subfamily than any other subfamily including the critical aspartate residue described earlier (Figures 1D and 8). Thus, ω-loop swap mutants of VanA and VanC2 were constructed with different amounts of the ω-loop from one enzyme replaced by the corresponding amino acids from the ω-loop of the other enzyme (Figure 8B).

(a) Portions of VanC2 ω-Loop Inserted into a VanA Template. The amino acids 240−255 of VanA were replaced by 249−260 of VanC2 to generate the small VanC2 loop swapped into VanA [VanAωC2(S)] (Figure 8B). When tested at pH 7.5 and 6.0, no detectable D-Ala-D-lactate was formed by this swap mutant, suggesting that the putative ω-loop of VanA is necessary for depsipeptide function. On the other hand, this mutant had improved dipeptide ligase activity over wild-type VanA (Table 6). The K_{M2} for D-Ala is reduced from 210 mM for the wild-type VanA enzyme at pH 7.5 to 34 mM for the swap mutant. However, the k_{cat} is reduced 2-fold, resulting in a 3-fold improvement in catalytic efficiency. Similarly, the K_{M2} for D-Ser is reduced from 34 to 6.3 mM at pH 7.5, which is close to the 1 mM K_{M2} value for wild-type His$_6$−VanC2, and the catalytic efficiency is improved 2-fold.

A larger portion of the VanC2 ω-loop (239−262) was substituted for 230−257 VanA [VanAωC2(L)] (Figure 8B). This mutant also failed to form D-Ala-D-lactate but had an improved dipeptide K_{M2} of 42 mM for D-Ala and 5.6 mM for D-Ser (Table 6), a similar result to the smaller loop swap version [VanAωC2(S)]. However, the k_{cat} values for this mutant were lowered an additional 10-fold compared to the previous swap mutant possibly due to improper orientation or positioning of the substituted amino acids. When stored

at 4 °C, this mutant started to precipitate after several days, indicating reduced stability of this enzyme so no further studies were conducted.

By replacing the putative ω-loop of VanA by that of VanC2, both the lysine residue proposed to stabilize the phosphoryl transfer transition state (Lys215 in DdlB, *21*) and the tyrosine residue (Tyr216 in DdlB, *17*) were imported (Figure 1D and 2). To see if the corresponding lysine (Lys246) in the hybrid ω-loop of VanAωC2(S) has a similar role, this residue was mutated to alanine in VanAωC2(S) and wild-type VanC2. The K255A VanC2 mutant had no detectable D-Ala-D-Ala ligase activity and had a 375-fold lower k_{cat} and a 16-fold higher K_{M2} as a D-Ala-D-Ser ligase (k_{cat}/K_{M2} down 6100-fold), suggesting that Lys255 is indeed necessary for efficient catalysis (Table 6). The corresponding Lys246 VanAωC2(S) mutation also affected K_{M2} by 14- and 13-fold for D-Ala_2 and D-Ser, respectively, possibly because of a disruption in the structure of the ω-loop. However, the K246A VanAωC2(S) mutant surprisingly retained the same rate of catalysis as VanAωC2(S) (87 vs 100 min^{-1}). This result implies that the VanA template of the swap mutant is using another mechanism to stabilize phosphoryl transfer and suggests that the mechanism used by VanA resides outside the ω-loop primary structure.

The loss of depsipeptide ligase activity in the VanAωC2-(S) swap mutant was further investigated by constructing the Y247F mutant, which corresponds to the Y216F DdlB mutant that gained some D-Ala-D-lactate ligase activity (*17*). Y247F VanAωC2(S) had a similar k_{cat} as VanAωC2(S) for D-Ala-D-Ala and D-Ala-D-Ser formation, but failed to regain depsipeptide activity at either pH 6.0 or 7.5 (Table 6). This result corresponds to the failure of Y256F VanC2 to form D-Ala-D-lactate (*37*) and supports a different mechanism for utilizing D-lactate as a substrate by VanA compared to LmDdl2 and Y216F DdlB.

(b) Portions of VanA ω-Loop Inserted into a VanC2 Template. Loop swap mutants were also done in the reverse direction by replacing the ω-loop of VanC2 with that of VanA to see if the putative ω-loop of VanA is sufficient for depsipeptide activity. The small loop version of VanA swapped into VanC2 [VanC2ωA(S)] consisted of residues 240−255 of VanA substituted for residues 249−260 of VanC2 (Figure 8B). For the large swap mutant, amino acids 230−255 of VanA replaced 239−260 of VanC2 [VanC2ωA-(L)] (Figure 8B). Two additional mutants were introduced into the VanC2ωA(L) swap mutant, H320Y and A325R, that were designed to convert residues in VanC2 predicted to be in contact with the ω-loop to those of VanA in case these residues were needed for favorable interactions with the introduced VanA ω-loop. These loop swap mutants failed to use D-lactate, D-hydroxybutyrate, or D-glyceric acid for depsipeptide formation, indicating that other residues are required for depsipeptide activity.

For VanC2ωA(S), the D-Ala-D-Ala and D-Ala-D-Ser activities did not saturate and were reduced 8- and 4800-fold in catalytic efficiency, respectively, compared to wild-type VanC2 (Table 6). In contrast, VanC2ωA(L) had no detectable ligase activity. Converting additional residues to the corresponding ones in VanA, giving the H320Y/A325R VanC2ωA(L) mutant, restored some dipeptide ligase activity, indicating that the two extra residues mutated are indeed important for the loop orientation. This mutant had a K_{M2} for D-Ser of 3.1 mM, which is comparable to wild-type VanC2 (1 mM K_{M2}); however, the k_{cat} was down 56-fold.

The ability of two of the swap mutants to retain 5−12% of the wild-type VanC2 D-Ala-D-Ala activity (Table 6) is somewhat unexpected because Lys255 is no longer present to stabilize phosphoryl transfer. In addition, a previously reported swap mutant with the ω-loop of DdlB (208−217) replaced by that of VanA (237−246) only retained 0.03% of the wild-type DdlB activity (*21*). To determine whether Arg251 or Lys260, which are not essential for VanA activity (corresponding to the Arg242 and Lys251 in VanA), are able to substitute for Lys255 in VanC2, the single and double R251A and K260A mutants in H320Y/A325R VanC2ωA-(L) were constructed. These mutants had no detectable activity, perhaps either because the lysine or arginine residues are necessary for activity or the enzymes were not properly folded.

DISCUSSION

A central molecular determinant of the VanA and VanB clinical phenotypes in vancomycin-resistant enterococci is the ability of VanA but not the homologous DdlB or VanC2 D-,D-ligases to activate D-lactate selectively over D-Ala_2 or D-Ser to capture the D-Ala-OPO_3^{2-} intermediate in the ligase active sites. Analysis of the gain of function depsipeptide ligase activity of VanA (and VanB) devolves to assessing the structural basis of functional discrimination of the D-α-hydroxy acid vs D-α-amino acid. Here we have focused on two approaches: (1) analysis of the pH dependence of D-lactate vs D-Ala_2 K_{M2} values and (2) mutagenesis of the region in VanA corresponding to the ω-loop region in DdlB and VanC2. To make the normal dipeptide product D-Ala-D-Ala, the D-Ala-D-X ligases have to activate two identical D-Ala molecules and differentiate them in reactivity, one as the N-terminal electrophile, the second as the C-terminal nucleophile in the peptide-bond-forming step. D-Ala_1 is targeted to be the electrophile by binding in a subsite of the ligase active site in proximity to the γ-phosphoryl group of bound ATP. An active-site lysine side chain (Lys215 in DdlB) and a Mg^{2+} ion coordinate the anionic substrates, shield charge, and facilitate PO_3^{2-} transfer to yield the mixed acyl-phosphoric anhydride D-alanyl-phosphate, with the carboxyl from D-Ala_1 now activated for transfer to nucleophiles. Then, the second D-alanine, D-Ala_2, has to be bound and deprotonated at the cationic NH_3^+ group to yield the free base NH_2 form that can function as the electron-rich nucleophile in the peptide-bond-forming step, the capture of D-Ala-OPO_3^{2-} (Scheme 1). We had previously suggested that *E. coli* DdlB might select the free base form of D-Ala_2 directly for binding, but the pH dependence of the D-Ala_2 K_{M2} (*17*) did not support that interpretation as noted by recent calculations (*44*) with only an 8-fold change in D-Ala_2 K_{M2} over the pH range 6.0−9.2 (*39*). On the other hand, our observations on the pH dependence of the D-Ala_2 K_{M2} value for the VanA ligase (*17*) indicated a steeper slope and that observation has been substantially extended in the work here on VanA.

The VanA D-Ala-D-X ligase is a much better depsipeptide ligase at low pH (e.g., pH 6−6.5) than a dipeptide ligase whereas at high pH (e.g., pH 8.5−9.0) the dipeptide product is much preferred. The switchover is largely a K_M effect,

driven by the pH dependence of the K_{M2} of D-Ala_2 but not of D-lactate, with the D-Ala_2 binding disfavored at low pH. We report in this paper that VanA, in contrast to DdlB ligase, increases catalytic efficiency selectively as a dipeptide ligase in parallel to the mole fraction of the free base form of D-Ala in solution. Thus, there is a 27-fold improvement in D-Ala_2 K_{M2} (270 to 10 mM) from pH 7.25 to 8.80. Since k_{cat} remains essentially constant, this translates into a corresponding improvement in the k_{cat}/K_{M2} catalytic efficiency ratio. Extrapolating to the limit defined by the pK_a of the amino group of alanine [pK_a of 9.87, (*38*)], the estimated K_{M2} of 0.66 mM for D-Ala_2 (as monanionic carboxylate) approaches that of the monoanionic D-lactate (0.69 mM) whose α-hydroxyl group does not titrate in the physiological pH range.

Further validation that VanA gains room to function as a D-Ala-D-lactate depsipeptide ligase by selectively discriminating against the predominant zwitterionic form of D-Ala (pK_a of 9.87) for binding productively to the D-Ala_2 subsite comes from a matching series of K_M vs pH curves for D-Ser (pK_a of 9.15), which show that the CH_2OH side chain in the D-X subsite is accommodated and that K_{M2} values again follow the titration curve of the α-ammonium group. When the CH_3 side chain of D-Ala_2 was changed by substitution of one, two, or three hydrogens by fluorines, there is very little effect on size of the side chain but tremendous through bond inductive effects on pK_a and now the lower pK_a of the amino groups have the predicted behavior for D-Ala-D-F-Ala, D-Ala-D-F_2-Ala, and D-Ala-D-F_3-Ala formation, by shifting the K_{M2} curves to lower pH. It does not appear that binding of the uncharged 2-NH_2 and 2-OH forms of D-Ala and D-lactate are affected by putative titrating of key side chains in the enzyme in this pH range, given the pH independent behavior of K_{M2} D-F_3-Ala and D-lactate.

It seems very likely then that the VanA and VanB D-,D-ligases in VRE have acquired the depsipeptide ligase gain of function activity by active discrimination against the bulk zwitterionic form of D-Ala when it is recruited to subsite 2, allowing D-lactate to compete effectively. Since the k_{cat} for reaction with the less nucleophilic hydroxyl is 17-fold lower (32 vs 550 min^{-1}) than with the free base form of D-Ala_2, D-lactate can win the competition only if it is recognized at a much lower concentration.

The question then arises how does this discrimination occur and why does it not happen in the DdlB and VanC (D-Ala-D-Ser) ligases. To date, we have obtained, via collaboration with the laboratory of Jim Knox at University of Connecticut, X-ray structures of the wild-type *E. coli* DdlB and the Y216F mutant ligases but there are no structures for the VanC subfamily or the VanA subfamily of D-,D-ligases (*20*, *46*). In the DdlB active site, the ω-loop region contains two residues (Lys215 and Tyr216) that are important for catalytic function. The ω-loop in the VanC D-Ala-D-Ser ligase subfamily and in the *Leuconsotoc mesenteroides* D-Ala-D-lactate ligase subfamily is highly homologous, but in the VanA subfamily, it shows no conservation in residue identity or residue number and in particular the Lys215 and Tyr216 equivalents were not obvious.

To evaluate potential loop function in VanA, we have mutated 14 residues to alanine in the 26 residue stretch of 230−255, to test any functional side chain in both dipeptide and depsipeptide ligase activity. Twelve of the 14 alanine mutants were equally efficient as wild-type VanA, serving as good controls for the two impaired mutants and consistent with this also being an unstructured loop region of the enzyme. The Asp232 acidic side chain appears to be particularly important for catalysis and could be a residue that coordinates an active-site Mg^{2+} or a water molecule involved in catalysis. There are three basic side chains, Arg242, His244, and Lys251, which seemed good candidates for cationic groups that could provide selective electrostatic repulsion to the zwitterionic D-Ala_2 but not D-lactate. Thus, pH profiles of catalytic efficiency were conducted with the three mutant VanA ligases, R242A, H244A, and K251A. The K251A shows a variation of log $1/K_{M2}$ vs pH of 0.99, very close to that of wild-type VanA (0.98) and the log of the mole fraction of the free amine at the same pH range 6.9−8.8 (0.98). The H244A is a marginally less step (0.82) while R242A (0.73) shows about half the decrease in K_{M2} value vs pH in the range evaluated. The double mutant R242A/H244A behaved essentially as the single R242A mutant, providing a second construct with lowered efficiency at rejecting the zwitterionic form of D-Ala_2. It would appear that the cationic side chain of Arg242 in a loop region of VanA, presumably unstructured in free enzyme, but closing over bound substrates in ES complexes could provide some of the rejection of the bulk form of D-Ala_2 by electrostatic repulsion. In addition, His244 could participate in the electrostatic repulsion either directly by repelling the NH_3^+ form of D-Ala_2 or indirectly by properly orienting Arg242. There is still a substantial residual K_{M2} vs pH effect in the R242A/H244A VanA double mutant, indicating additional determinants of D-Ala_2 zwitterion discrimination remain uncharacterized. Since the active site of VanA can still actively reject the NH_3^+ form of D-Ala_2 at pHs up to 8.8, it is most likely that another charged residue that does not titrate in the pH range examined, such as, arginines and lysines, and/or the presence of a nearby metal atom also plays a role in rejecting the protonated amine.

The H244A VanA mutant was also intriguing in that it was selectively disabled as a depsipeptide ligase (150-fold lower k_{cat}/K_{M2}) while dipeptide ligase catalytic efficiency increased 2-fold. The 300-fold selectivity suggests the side chain of His244 may have a specific activating effect on the D-lactate reaction. Given that D-lactate needs its 2-OH group to be deprotonated in the depsipeptide-bond-forming transition state but the free base form of D-Ala_2 does not in the analogous dipeptide-bond-forming transition state, it may be that His244 can either function as catalytic base or orient a bound water molecule to assist in D-lactate alkoxide equivalent generation.

The counterpart of Lys215 in *E. coli* DdlB (Figure 2), the cationic side chain that is crucial for catalysis of the γ-phosphoryl transfer step from ATP to D-Ala_1 to yield the aminoacyl−phosphate intermediate, is not yet identified. When the other conserved lysine and arginine residues among the VanA ligase family, not mutated in this work, are compared and mapped onto the X-ray structure of *E. coli* DdlB as a predictive model, none are found close to the active site. Such a lysine, to shield charge and orient the transferring γ-PO_3, is a fixture of kinase and ligase active sites and it may be that the VanA folds to bring a lysine from an unanticipated region of primary sequence into the active site. It is also possible that an additional (third) magnesium atom fulfills the lysine role.

In addition to the point mutations in VanA, we also constructed putative loop swaps, moving the VanC2 ω-loop into the VanA template and the reciprocal VanA loop into the VanC2 template. The VanC2 loop into the VanA template was perhaps the more revealing in that this chimeric VanA ligase had a 6-fold improvement in D-Ala_2 K_{M2} (220 mM down to 34 mM) and also D-Ser K_{M2} (34 mM to 6 mM). Since k_{cat} dropped 2-fold, this chimeric VanA was a 3-fold better D-Ala-D-Ala ligase by catalytic efficiency ratio, suggesting that the functional active-site geometry was intact, but the discrimination against the zwitterionic D-X amino acids was lessened, as anticipated for a VanC-type ligase. This result supports the possibility that VanA could have evolved from a VanC framework. Moreover, all depsipeptide ligase activity was lost, arguing for the crucial role of the VanA loop in D-lactate selection. In addition, mutation of Lys246 in the VanC2 ω-loop of VanAωC(S) did not effect the dipeptide ligase k_{cat} values; however, the corresponding mutation in wild-type VanC2 lowered the D-Ala-D-Ser k_{cat} value 375-fold. This result further supports the different mechanisms used by VanC2 and VanA to stabilize phosphoryl transfer. The swap of the VanA ω-loop into the VanC2 template did not enable depsipeptide ligase activity so not all the active-site features are reproduced in that chimera.

In conclusion, the D-,D-ligase subfamilies represented by Ddl and VanC2 on one hand (dipeptide ligases only) and by VanA and VanB on the other hand (dipeptide and depsipeptide ligases) have evolved to show dramatically different K_{M2} values for D-Ala_2. *E. coli* DdlB has a K_{M2} of 2 mM (*39*) while VanA has a K_{M2} of 210 mM at pH 7.5. This 105-fold negative selection by VanA reflects discrimination against productive binding of the zwitterionic form of D-Ala_2. Since the free base form represents only about 0.1% of the bulk D-alanine species at neutral pH, D-lactate can compete effectively for binding and capture of the bound D-Ala_1−OPO_3^{2-} intermediate. When the K_{M2} for D-Ala_2 is corrected for the free base form, it falls to the 0.6−0.7 mM value seen for D-lactate, suggesting equivalent competition of the monoanionic forms of D-lactate and D-Ala_2, at which point the amine is the better nucleophile. The structural basis of discrimination against the D-Ala_2 zwitterion, peculiar to VanA and VanB, is still unknown and will probably require an X-ray structure with bound substrates or transition state analogues to immobilize the active-site loop, but it is likely that the cationic side chain of Arg242 in VanA contributes an electrostatic repulsion to D-Ala_2 zwitterion.

ACKNOWLEDGMENT

We are grateful to Merck and Co (Rahway) for providing us with the D-F_2-Ala substrate. We thank Sven G. Hyberts for communicating the predicted three-dimensional structure model of VanB. We thank Thomas A. Keating, Florian Hollfelder, and other members of the Walsh laboratory for helpful discussions. I.A.D.L. wishes to acknowledge the Medical Research Council of Canada for Postdoctoral Fellowship support. V.L.H. is a Howard Hughes Medical Institute Fellow.

REFERENCES

1. Neu, H. C. (1992) *Science 257*, 1063−1073.
2. Tomasz, A. (1994) *N. Engl. J. Med. 330*, 1247−1251.
3. Swartz, M. N. (1994) *Proc. Natl. Acad. Sci. 91*, 2420−2427.
4. Kirst, H. A., Thompson, D. G., and Nicas, T. I. (1998) *Anticmicrob. Agents Chemother. 42*, 1303−1304.
5. Moellering, R. C., Jr. (1991) *J. Antimicrob. Chemother. 28*, 1−12.
6. Moellering, R. C. J., and Gold, H. S. (1996) *N. Engl. J. Med. 335*, 1445−1453.
7. Arthur, M., Depardieu, F., Reynolds, P., and Courvalin, P. (1996) *Mol. Microbiol. 21*, 33−44.
8. Bugg, T. D., Wright, G. D., Dutka-Malen, S., Arthur, M., Courvalin, P., and Walsh, C. T. (1991) *Biochemistry 30*, 10408−10415.
9. Arthur, M., and Courvalin, P. (1993) *Antimicrob. Agents Chemother. 37*, 1563−1571.
10. Reynolds, P. E., Depardieu, F., Dutka-Malen, S., Arthur, M., and Courvalin, P. (1994) *Mol. Microbiol. 13*, 1065−1070.
11. Walsh, C. T., Fisher, S. L., Park, I. S., Prahalad, M., and Wu, Z. (1996) *Chem. Biol. 3*, 21−28.
12. Wright, G. D., Holman, T. R., and Walsh, C. T. (1993) *Antimicrob. Agents Chemother. 36*, 1514−1518.
13. Barna, J. C. J., and Williams, D. H. (1984) *Annu. Rev. Microbiol. 38*, 339−357.
14. Reynolds, P. E., Snaith, H. A., Maguire, A. J., Dutka-Malen, S., and Courvalin, P. (1994) *Biochem. J. 301*, 5−8.
15. Billot-Klein, D., Blanot, D., Gutmann, L., and van Heijenoort, J. (1994) *Biochem. J. 304*, 1021−1022.
16. Dutka-Malen, S., Molinas, C., Arthur, M., and Courvalin, P. (1992) *Gene 112*, 53−58.
17. Park, I. S., and Walsh, C. T. (1997) *J. Biol. Chem. 272*, 9210−9214.
18. Meziane-Cherif, D., Badet-Denisot, M. A., Evers, S., Courvalin, P., and Badet, B. (1994) *FEBS Lett. 354*, 140−2.
19. Park, I. S., Lin, C., and Walsh, C. T. (1997) *Proc. Natl. Acad. Sci. 94*, 10040−10044.
20. Fan, C., Moews, P. C., Walsh, C. T., and Knox, J. R. (1994) *Science 266*, 439−443.
21. Shi, Y., and Walsh, C. T. (1995) *Biochemistry 34*, 2768−2776.
22. Sambrook, J., Fritsch, E. F., and Maniatis, T. (1989) Molecular Cloning: A Laboratory Manual. 2nd ed., Cold Spring Harbor Laboratory, Plainview, NY.
23. Saiki, R. K., Gelfand, D. H., Stoffel, S., Scharf, S. J., Higuchi, R., Horn, G. T., Mullis, K. B., and Erlich, H. A. (1988) *Science 239*, 487−491.
24. Saiki, R. K., Scharf, S., Faloona, F., Mullis, K. B., Horn, G. T., Erlich, H. A., and Arnheim, N. (1985) *Science 230*, 1350−1354.
25. Lessard, I. A. D., and Perham, R. N. (1994) *J. Bio. Chem. 269*, 10378−10383.
26. Ho, S. N., Hunt, H. D., Horton, R. M., Pullen, J. K., and Pease, L. R. (1989) *Gene 77*, 51−59.
27. Edelhoch, H. (1967) *Biochemistry 6*, 1948−1954.
28. Pace, C. N., Yajdos, F., Fee, L., Grimsley, G., and Gray, T. (1995) *Protein Sci. 4*, 2411−2423.
29. Laemmli, U. K. (1970) *Nature 227*.
30. Daub, E., Zawadzke, L. E., Botstein, D., and Walsh, C. T. (1988) *Biochemistry 27*, 3701−3708.
31. Neuhaus, F. C. (1962) *J. Biol. Chem. 237*, 3128−3135.
32. Neuhaus, F. C. (1962) *J. Biol. Chem. 237*, 778−786.
33. Segel, I. H. (1975) *Enzyme Kinetics*, Wiley, London.
34. Zawadzke, L. E., Bugg, T. D., and Walsh, C. T. (1991) *Biochemistry 30*, 1673−1682.
35. Bugg, T. D., Dutka-Malen, S., Arthur, M., Courvalin, P., and Walsh, C. T. (1991) *Biochemistry 30*, 2017−2021.
36. Randerath, K., and Randerath, E. (1964) *J. Chromatogr. 16*, 111−125.
37. Healy, V. L., Park, I. S., and Walsh, C. T. (1998) *Chem. Biol. 5*, 197−207.
38. *The Merck Index* (1996) 12th ed., Merck & Co., Inc., Whitehouse Station, NJ.
39. Park, I. S., Lin, C. H., and Walsh, C. T. (1996) *Biochemistry 35*, 10464−10471.
40. Wang, E. A., and Walsh, C. T. (1981) *Biochemistry 20*, 7539−7546.

41. Havel, T. F., and Snow, M. E. (1991) *J. Mol. Biol. 217*, 1−7.
42. Kato, H., Tanaka, T., Yamaguchi, H., Hara, T., Nishioka, T., Katsube, Y., and Oda, J. (1994) *Biochemistry 33*, 4995−4999.
43. Marolewski, A. E., Mattia, K. M., Warren, M. S., and Benkovic, S. J. (1997) *Biochemistry 36*, 6709−6716.
44. Carlson, H. A., Briggs, J. M., and McCammon, J. A. (1999) *J. Med. Chem. 42*, 109−117.
45. Marshall, C. G., Broadhead, G., Leskiw, B. K., and Wright, G. D. (1997) *Proc. Natl. Acad. Sci. 94*, 6480−6483.
46. Fan, C., Park, I. S., Walsh, C. T., and Knox, J. R. (1997) *Biochemistry 36*, 2531−2538.
47. Thompson, J. D., Higgins, D. G., and Gibson, T. J. (1994) *Nucleic Acids Res. 22*, 4673−4680.

BI991384C